QATAR UNIVERSITY

COLLEGE OF HEALTH SCIENCE

VASCULAR ENDOTHELIAL DYSFUNCTION AS THE MECHANISM FOR DEVELOPMENT OF OBESITY

BY

RAJA'A SALEH DALLOUL

A Thesis Submitted to the Faculty of

the College of Health Science

in Partial Fulfillment

of the Requirements

for the Degree of

Master of Science

in Biomedical

Laboratory Sciences

June 2018

COMMITTEE PAGE

The members of the Committee approve the thesis of Raja'a Dalloul

defended on 20/05/2018.

_____

Dr. Ahmed Malki
Thesis/Dissertation Supervisor

_____

Dr. Nasrin Mesaeli
Committee Member

_____

Dr. Gianfranco Pintus
Committee Member

_____

Committee Member

Approved:

_____

Asma Al-Thani, Dean, College of Health Science

ABSTRACT

Obesity is one of the major public health issues in the world with a rapid increase in its prevalence. According to the last public health report from supreme public health in Qatar in 2012, 71.8 % of the women were overweight compared to 68.3% of men. Adipocytes are where their size can vary with different food intake. The rapid expansion of the adipose tissue requires high vascularization to support their expansion. Branching of vasculature depends on properly functioning endothelial cells of the vessels. Different diseases including diabetes and obesity has been reported to cause defects in the endothelial cell function. This defect could be due to changes in nitric oxide production which regulate vascular contractility or production of other oxyradicals leading to damage to the tissue.

Calreticulin (CRT) is a multifunctional protein localized in the endoplasmic reticulum of all mammalian cells. The main functions of CRT are regulation of intracellular Ca^{2+} hemostasis and chaperone. Our transgenic mouse model overexpressing CRT in endothelial cells (EC^{CRT+}) showed evidence of endothelial dysfunction and susceptibility to obesity and diabetes as they age. Therefore, we hypothesized that overexpression of CRT in endothelial cells results in endothelial dysfunction that increases angiogenesis leading to activation of adipogenesis.

In our study we examined changes in the phenotype of adipocytes of wild type (*wt*) and EC^{CRT+} mice fed either high fat (60%) or regular fat (10%) diet for different time points (8-24 weeks). Our results illustrated that these mice expressed lower eNOS thus leading to endothelial dysfunction. The Glucose tolerance test (GTT) assay illustrated that

EC^{CRT+} mice developed diabetes as they aged when on 10% fat diet. However, on high fat diet they failed to regulate blood glucose even at 8 weeks. Histological analysis of the *wt* and *EC*$^{CRT+}$ mice showed significant changes in the adipocyte size and number suggesting a possible association between endothelial dysfunction and adipogenesis. Our study is the first to show an important role of endothelial dysfunction in altering adipogenesis process leading to the development of obesity and diabetes. Our data also highlights the importance of an endoplasmic reticulum chaperone in this process.

DEDICATION

To those people who made their dreams come true.

To the strongest people I've ever learned from.

TO MY FATHER & MY MOTHER

ACKNOWLEDGMENTS

I would like to thank Dr. Ahmed Malki, Associate Dean for Academic Affairs, for his support and encouragements.

The decision of applying to the master program was never possible without the support of my team at Weill Cornell Medicine-Qatar.

I would like to thank Dr. Nasrin Mesaeli, Associate Professor of Biochemistry and Dr. Hamid Massaeli for their great support, encouragement and all their guidance and supervision throughout the course of my master study. Thank you for making me feel more independent, for teaching and giving me from your heart.

My sincere thanks also go to all my colleagues at the lab for being ever kind to show interest in my research and surrounding me with care and a cordial working environment.

My greatest gratitude goes to my friends for their friendship, support and for being next to me whenever I need their help and encouragement, thank you Ayeda Ahmed and Noor al-Hajri for being such a support during the hard and good times.

Finally, my deepest gratitude goes to my family for their unflagging love and unconditional support throughout my life and my studies.

TABLE OF CONTENT

LIST OF TABLES

LIST OF FIGURES

LIST OF ABREVIATION

ATE	Arginyl-tRNA Protein Transferase
Bip	Immunoglobulin Heavy Chain Protein
Ca^{2+}	Calcium
Cad	Cadherin
CRT	Calreticulin
cDNA	Complementary Deoxyribonucleic Acid
CEBPα	CCAAT Enhancer-Binding Protein Alpha
DEPC	Diethyl Pyrocarbonate
DAPI	4',6-diamidino-2-phenylindole
EC^{CRT+}	Endothelial Cell Overexpressed Calreticulin
ECM	Extracellular Matrix
eNOS	Enzyme Nitric Oxide Synthase
ER	Endoplasmic Reticulum
ERAD	Endoplasmic Reticulum Associated Degradation
ESC	Embryonic Stem Cells
FGF	Fibroblast Growth Factor
GTT	Glucose Tolerance Test
HA-tagged	Hemagglutinin Tagged
HUVEC	Human umbilical vein endothelial cells
IP_3	Inositol Triphosphate
KDa	Kilo Dalton

KDEL	ER retention Signal
mRNA	Messenger Ribonucleic Acid
NO	Nitric Oxide
NHS	National Health Strategy
PBS	Phosphate Buffered Saline
PCR	Polymerase Chain Reaction
PDI	Disulfide Isomerase
PPARγ	Peroxisome Proliferator-Activated Receptor Gamma
qRT-PCR.	Quantitative Reverse Transcriptase Polymerase Chain Reaction
RAP	Receptor Associated Proteins
ROS	Reactive Oxygen Species
SERCA	Sarco-Endoplasmic Reticulum Ca^{2+} Atpase
TG	Triacylglycerol
TSP-1	Thrombospondin-1
UPR	Unfolded Protein Response
VEGF	Vascular Endothelial Growth Factor
WCM-Q	Weill Cornell Medicine in Qatar
WHO	World Health Organization
wt	Wild-Type

CHAPTER 1: INTRODUCTION

Obesity is considered as one of the major public health issues in the world with a rapid increase in its prevalence reaching an epidemic proportion (Lobato et al., 2012). In the last WHO report published in 2012, 1.9 billion of adults 18 years and older, and 43 million children under 5 years, were reported to be overweight. The same report illustrated that in total 13% of the adult population are obese, with higher percentage in women (15%) compared to men (11%) (WHO, 2012). Not only western countries suffer from obesity, gulf region also have a high prevalence of overweight and obesity among their population. According to the last public health report from supreme public health in Qatar in 2012, 71.8 % of the men were overweight compared to 68.3% of women (Figure1.1). Among the gulf region, Qatar has the 6th highest rate of obesity in young boys (NHS, 2012). Moreover, the WHO survey in 2009 showed 70% of the Qatari children were obese because of the nutritional changes and unhealthy lifestyle (Figure 1.2). Many of the published studies illustrate the role of obesity in developing various diseases such as atherosclerosis, hypertension, insulin resistance, non-alcoholic fatty liver and cancer, all of which increase the rate of mortality and morbidity worldwide (Chan & Woo, 2010).

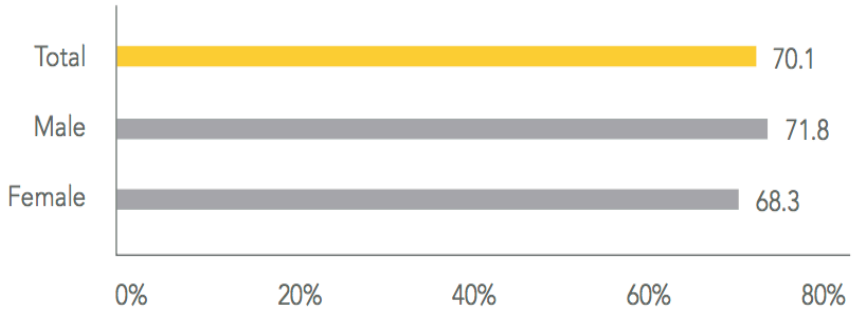

Figure 1.1 Qatar National Health Report released in 2012, statistics showing the prevalence of overweight and obesity among Qatari populations (NHS, 2012).

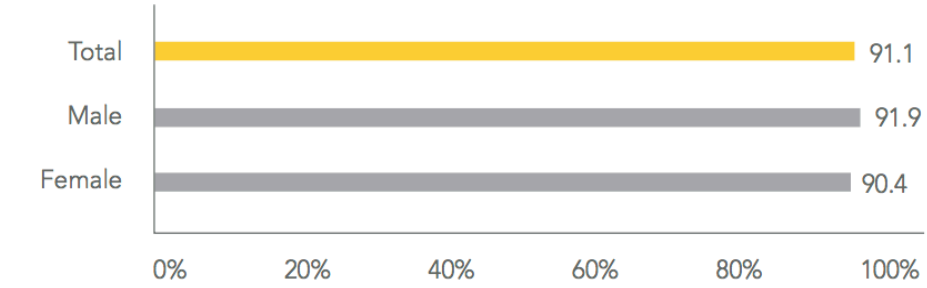

Figure 1.2 Qatar National Health Report released in 2012, statistics showing the prevalence of poor nutrition among Qatari population (NHS, 2012).

Adipose tissue is an important endocrine organ that maintains body energy hemostasis (Caruso, Balistreri, & Candore, 2010) (Trayhurn & Beattie, 2001). Adipocytes are active cells secreting a number of adipokines such as adiponectin, leptin and resistin that modulate cell metabolism. During normal development, pre-adipocytes undergo a process of differentiation which is known as adipogenesis. During high caloric intake, the size of adipocytes increase to facilitate the storage of excess product as lipid. The growing adipose tissue requires higher supply of oxygen and nutrients, that will be achieved through increasing the number or branching of the pre-existing vasculature (Lijnen, 2008, Bruemmer, 2012).

Angiogenesis is defined as the growth of new blood vessels from pre-existing vessels within the tissues (Corvera & Gealekman, 2014). Angiogenesis is considered a significant process for tissue development, in adipose tissue it is important for adipose tissue expansion, in tumor progression it allows growth of the solid mass and provides means for metastasis and during wound healing it is essential for closure of the wound. Thus, improper angiogenesis could cause adipose tissue dysfunction, endothelial dysfunction and improper adipogenesis in obesity (Kolluru, Bir, & Kevil, 2012).

A layer of endothelial cells covers the entire lumen side of the vasculature. Endothelium layer forms the barrier that separates the vessel wall from the blood. Vascular endothelium is a dynamic tissue that produces many factors therefore playing a significant role in controlling vascular tone, maintenance of blood circulation, controlling the blood coagulation and inflammatory responses (Avogaro & De Kreutzenberg, 2005).

Endothelial dysfunction is the inability of endothelium to maintain the vascular homeostasis. It is defined as the imbalance in the production of vasodilator and vasoconstrictor substances that are produced by the endothelium (Lobato et al., 2012). Endothelial cells mainly produce nitric oxide through the activity of its nitric oxide synthase (eNOS). Endothelial dysfunction could develop due to reduction of nitric oxide bioavailability that results from impaired endothelium layer and/or increased nitric oxide inactivation by reactive oxygen species (ROS) (Singhal, 2005). Endothelial dysfunction causes inability of the arteries and arterioles to ideally dilate in response to a proper stimulus by vasodilator on the endothelium (Witting et al., 2007).

Previous studies suggested that Calreticulin (CRT) could play a role in vascular development. Mesaeli et al., 1999, showed that during mice development, CRT protein was highly expressed in early stages of heart and vascular development (Mesaeli et al., 1999). CRT promoter activity within the heart and descending aorta suggest that CRT could have a role in regulating the formation of new blood vessels in mice (Mesaeli et al., 1999). Originally, CRT was identified as universal Ca^{2+} binding protein located in the lumen of endoplasmic reticulum (ER). It has many vital functions including regulation of Ca^{+2} homeostasis, chaperoning in ER and cell adhesion. CRT as one of the ER chaperone proteins, binds to the newly synthesized proteins and supports them for correct tertiary structure folding (Yokoyama & Hirata, 2005). Various studies discussed the importance of CRT, however its role in the development of endothelial dysfunction has not been fully discussed.

Several studies showed that endothelial dysfunction can result as a consequence of many diseases such as diabetes, obesity and hypertension and showed that increased adipocyte angiogenesis affects the development of obesity (Corvera & Gealekman, 2014)(Neels, et al., 2004) but it is not clear how endothelial dysfunction could affect the onset of obesity. Therefore, my study focuses on this aspect.

1.1 HYPOTHESIS

Overexpression of CRT in endothelial cells results in endothelial dysfunction which affects the process of angiogenesis and adipogenesis leading to the development of obesity.

1.2 SIGNIFICANCE OF THE PROBLEM

Obesity has reached a worldwide epidemic status. It can result in the onset of many other diseases such as diabetes, cardiovascular disease and cancer. It is important to identify the cellular mechanism of development of obesity. The published literature has illustrated the onset of endothelial dysfunction as the result of obesity and diabetes. As part of Dr. Mesaeli's ongoing research on vascular development, an endothelial targeted transgenic mouse line was generated in her lab by overexpressing CRT, an ER chaperone, in these cells [will be referred to as (EC^{CRT+})]. One of the major phenotype of these mice is the development of visceral obesity and diabetes.

The preliminary results from Dr. Mesaeli's lab illustrated that these mice suffer from endothelial dysfunction. This mouse model highlighted the possible role of endothelial dysfunction in the development of diabetes and obesity. Thus, this mouse model provides a valuable tool to examine the cause and effect relationship between endothelial dysfunction and obesity. Initial histological analysis of the fat from these EC^{CRT+} mice showed changes in adipocyte size and number suggesting a possible association between endothelial dysfunction and adipogenesis. However, the exact mechanism of adipogenesis upon endothelial dysfunction and its correlation with CRT is not clear.

1.3 AIMS AND OBJECTIVES

AIM

Many studies have focused on how obesity induces endothelial dysfunction. Very little information is available on the *vice-versa*. Therefore, the aim of our study is to determine the cause and effect relationship between CRT, endothelial dysfunction and the development of obesity using the EC^{CRT+} mouse model.

OBJECTIVES

1. Characterization of adipocyte phenotype of EC^{CRT+} mice.
2. Examine Endothelial dysfunction.
3. Examine adipose tissue angiogenesis in EC^{CRT+} mice.
4. Determine effect of high fat diet on EC^{CRT+} adipocyte phenotype.

CHAPTER 2. REVIEW OF THE LITERATURE

2.1 Calreticulin

2.1.1 Calreticulin overview

Originally CRT was identified as a calcium (Ca^{2+}) binding protein that was isolated from endoplasmic reticulum (ER) of rabbit skeletal muscles (Ostwald & MacLennan, 1974). In 1989, the coding gene of this protein was cloned and named Calreticulin (CRT), showing the localization and functional characteristic of this protein (Mesaeli et al., 1999) (Michalak et al., 1999). The predicted molecular weight of CRT is 46 KDa but it appears as a 62 KDa protein on SDS-acrylamide gel due to high number of acidic amino acids at the C terminus of the protein (Michalak et al., 1999). Initial studies showed the localization of CRT to the ER but some reports also suggested its localization on the surface and in the nucleus of the cells (Wada et al., 1995) (Dupuis et al., 1993) (White, Zhu, & Tanzer, 1995) (Dedhar, 1994) (Arnaudeau et al., 2002). This is still a controversial topic in the field and more studies in intact cells and sophisticated imaging techniques needs to be conducted to confirm the other localization of the protein.

In addition to the regulation of Ca^{2+} homeostasis, CRT also functions as an ER lectin like chaperone. CRT as one of the chaperone proteins in the ER, binds to newly synthesized proteins and support their correct tertiary structure folding (Yokoyama & Hirata, 2005). CRT has been shown to be involved in ER stress and injury response (Hebert & Molinari, 2007) (Jeffery et al., Raghavan, 2011). Furthermore, it was shown that CRT is involved in the regulation of cell migration, and adhesion (Gold et al., 2010).

2.1.2 Structure

CRT gene in human is composed of 9 exons and 8 introns (Yokoyama & Hirata, 2005). It is located on chromosome 19 in human and chromosome 8 in mice (Rooke et al., 1997) (McCauliffe et al., 1992). Although forming 3-D structure for CRT has been challenging due to the inability to crystalize the protein, its conformation has been identified using X-ray structure (Michalak, et al., 2002)(Giraldo et al., 2010). CRT has three structural domains including, N-terminal domain that is important in protein-protein interaction, Proline-rich area known as P domain with internal repeats that is involved in protein-protein interaction and also binds Ca^{2+}, and the C-terminal domain which has a vital role in regulating Ca^{2+} homeostasis and ends with KDEL (Lys-Asp-Glu-Leu) retention signal of ER and (Jiang et al., 2014) (Figure 2.1).

The N-domain and P-domain of CRT share high homology to N and P domains of calnexin and based on this similarity it has been predicted to have a globular structure (Roderick, et al., 2000). N-terminus is also called lectin domain due to its binding to carbohydrate residues on the newly synthesized peptides (Schrag et al., 2001). The P domain contains tandem repeats of two proline rich sequence motifs which interact with one another in a head-to-tail fashion (Schrag et al., 2001). The structural similarities of the P domain between the CRT and calnexin was confirmed using NMR reconstruction (Leach et al., 2002). Moreover, the primary polypeptide and carbohydrate binding site of N-domain of CRT along with the P-domain, is responsible for the chaperone function of CRT (Leach et al., 2002).

The C-domain of CRT contains a large number of acidic amino acid residues (glutamic acids) that are characterized by their ability to bind Ca^{2+} with high capacity and low affinity (Baksh & Michalak, 1991). The C-domain is considered highly susceptible to proteolytic cleavage due to the lack of complex tertiary structure (Jorgensen et al., 2005). The highly negative charge of this domain has prevented the ability to crystalize CRT and obtain the full protein crystal structure. CRT has been shown to be phosphorylated on serine-threonine residues and arginylated by arginyl-tRNA protein transferase at the cell surface that increases susceptibility of the cell to apoptosis (Decca et al., 2007).

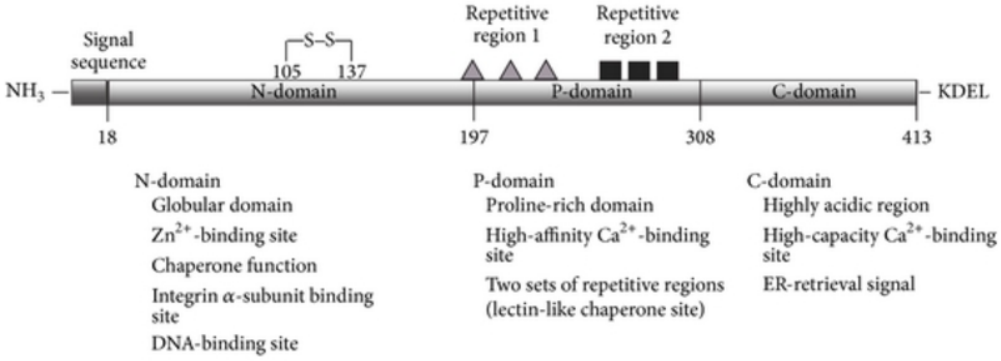

Figure 2.1 Schematic representation of the structural domains of calreticulin protein. The protein consists of three functional domains including: N-domain, P-domain, and C-domain. The KDEL ER retentional peptide at C-terminal and signal sequence at N-terminal. Modified figure from (Michalak et al., 1999).

2.1.3 Function

2.1.3.1 Calreticulin as Chaperone

The complex structure of CRT demonstrates how it can have several functions in and out of the cell, as a chaperone and as a regulator for the quality of the newly synthesized proteins (Michalak et al.,2009). ER is the place where polypeptides interact with the molecular chaperones and thiol oxidoreductases after translation. Inside the ER, chaperones are grouped according to their functions. Lectin chaperones such as Calnexin and CRT are involved in recognizing and folding the proteins that contain certain pattern of sugar moieties. Classical ER chaperones, includes several subfamilies, such as Hsps (40, 60, 70, 90, and 100 KDa) that are transcribed by the induction with heat shock. Another subfamily known as GRP78/BiP and Grp94 are glucose regulated proteins (Spiro et al.,1996) (Helenius, 2001).

In ER, some proteins can fold using general chaperones, however, due to the complex structure of some proteins, they require special assistance. This assistance is provided through chaperones known as substrate specific chaperones, which include receptor associated proteins (RAP) that ensure the proper folding of proteins and prevent the aggregation of low density lipoprotein receptors (Hebert & Molinari, 2007). Hsp47 which is a collagen specific chaperone is required for retaining the triple helical structure of collagen by interacting with other chaperones such as CRT and Calnexin (Spiro et al., 1996).

2.1.3.2 Calreticulin/Calnexin cycle

Calnexin and CRT are homologous lectin chaperones that interact with the newly synthesized glycoproteins in the ER. In fact, the role of this cycle is to selectively engage newly synthesized glycoproteins. The functional process of these chaperones starts once the polypeptide is recognized by CRT and calnexin to ensure the proper folding of these proteins through the cycle. Prolonged interaction between the protein and calnexin/CRT, will subject the protein to degradation via ER associated degradation (ERAD)(Hebert & Molinari, 2007). On the other hand, proper folding of proteins will allow them to be transported out the ER to the Golgi apparatus for further processing.

Glycosylation of newly synthesized proteins acts as a signal for enhanced folding and quality control and/or for the degradation of misfolded proteins (Hebert & Molinari, 2007). CRT, which is a soluble protein, associates with glycans that emerge deeper into the ER lumen while calnexin binds to glycans found in the membrane proximal domains (Trombetta et al.,1996). Calnexin binds transiently to most glycoproteins whereas CRT binds to a more restricted set of glycoproteins (Keller et al., 1998) (Peterson et al., 1995). Given that calnexin and CRT bind monoglucosylated glycans with micromolar affinities, their chaperone binding cycles are controlled via the glucosidases and glucose-transferase that dictate the composition of the carbohydrate on the maturing glycoproteins in the ER (Kapoor et al., 2003).

Monoglucosylated N-glycans mediate initial association of folding polypeptides with calnexin and/or CRT that exposes them to the glycoprotein dedicated oxidoreductase ERp57 (Hammond et al., 1994). ERp57 is an additional component in the calnexin/CRT cycle. It is a member of the PDI family of proteins (Oliver et al., 1997). ERp57 catalyzes rearrangements of disulfide-bonds within the substrate proteins, but does not recognize their glycon moiety (Zapun et al., 1998). It is likely that most glycopolypeptides are released from calnexin/CRT/ERp57 in a native, transport competent state (Frickel et al., 2002). They are rapidly deglucosylated and partially demannosylated and eventually sequestered in transport vesicles that leave the ER (Hebert & Molinari, 2007). For a fraction of the newly synthesized glycoproteins, folding is not completed in a single round of association with calnexin/CRT. The folding intermediate released from the lectin chaperones is deglucosylated, but its forward transport is inhibited by glucose transferase 1. Glucose transferase 1 adds back a glucose residue only to glycoproteins with nearly native conformation. These rebind to calnexin/CRT and are subjected to additional folding attempts likely to consist in disulfide reshuffling. Glycopolypeptides released from calnexin/CRT and displaying major folding defects are ignored by glucose transferase 1, rather, they attract BiP (Julio et al., 2004). They are extensively demannosylated and dislocated across the ER membrane for proteasome mediated degradation (Caramelo et al., 2003).

A study conducted by Pipe and colleagues demonstrated that some coagulation factors binds to different chaperones despite the structural similarity or glycosylation patterns. For instance, factor VIII interacts only with calnexin while Factor V interacts with both CRT and calnexin. In addition, CRT knockout cells (or CRT deficient) cells was shown to have a slight decrease in folding efficiency while cells with calnexin deficiency completely prevents folding of some proteins, such as hemagglutinin (Pipe et al.,1998). Moreover, CRT deficient cells have increased calnexin similarly calnexin deficient cells express higher level of CRT suggesting that these chaperones can compensate each other's function (Molinari et al., 2004). Remarkably, both CRT and calnexin knockout cells express higher levels of GRP78 which is known as the master regulator of the ER stress, suggesting that other ER chaperones may be compensating for the loss of CRT or calnexin, at least *in vitro* (Molinari et al., 2004). However, deletion of CRT system *in vivo* has been shown to cause embryonic death resulted from a lesion in cardiac development as shown by Mesaeli *et al.* (Mesaeli et al., 1999). A study conducted by Kraus, *et al.* in 2010 showed that calnexin knockout mice suffer from myelinopathy with no apparent effects on other systems (Kraus et al., 2010). However, Denzel *et al,* showed that calnexin deletion caused severe growth and motor disorders, and premature death (Denzel et al., 2002). These lethal outcomes could confirm that the calnexin/CRT chaperone system plays a vital role during protein biogenesis which may be restricted to specific organs or developmental phases.

2.1.3.3 Calreticulin and Ca^{2+} homeostasis

CRT plays a vital role in Ca^{2+} homeostasis within the cell (Wada et al., 1995). Ca^{2+} signaling is very important in regulating cell signaling, cell survival, induction of ER stress and apoptosis (Michalak et al., 2009). Therefore, it is crucial that ER and cytoplasmic Ca^{2+} are well controlled. The level of Ca^{2+} is sustained by an on/off stimulus which promotes Ca^{2+} uptake and release in the cytoplasm. The regulation of cytoplasmic Ca^{2+} is operated through different channels such as; receptor operated channels and inositol triphosphate (IP_3)(Berridge et al., 2000a). Once Ca^{2+} is released from these channels, it will be removed from the cytoplasm through sarco-endoplasmic reticulum Ca^{2+} ATPase (known as SERCA pump) into the ER. Following the reuptake, Ca^{2+} in the ER can be either free or bound to Ca^{2+} binding proteins (including many chaperons) such as CRT since it has high Ca^{2+} binding capacity (Berridge et al., 2000b).

Reduction in CRT level, decreases the capacity of Ca^{2+} storage of the cells that leads to accumulation of misfolded proteins, inhibition of ER Golgi trafficking which affects chaperone's functions (Peters & Raghavan, 2011). On the other hand, several studies demonstrated that overexpression of CRT increase the Ca^{2+} storage in the ER with no effect on the cytoplasmic Ca^{+2} level (Opas et al., 1996). For instance, Mery *et al.,* showed that CRT overexpression in L fibroblast cell lines increased Ca^{2+} content by 1.5+_0.2 fold (Mery et al., 1996). Furthermore, Arnaudeau et al., demonstrated that overexpression of CRT increased the luminal Ca^{2+} level in ER because of enhanced Ca^{2+} binding to its C-domain (Arnaudeau et al., 2002). These authors suggested a correlation between ER and mitochondria in some disease state that decreases the mitochondrial Ca^{2+} content and membrane potential in CRT overexpressing cells (Arnaudeau et al., 2002).

In addition, overexpression of CRT has been reported to enhance the inactivation and degradation of SERCA2a in cells under oxidative stress, suggesting a role for CRT regulation of Ca^{2+} homeostasis in the onset of myocardial disease (Ihara et al., 2005).

2.1.3.4 Calreticulin and ER stress

As previously mentioned, CRT is one of the ER chaperone proteins that works to ensure the proper folding of the newly synthesized proteins and their transportation from the ER into their final destination within the cell. Equilibrium in the cell is achieved between the nascent polypeptide numbers and ER chaperone numbers that are available to assist in folding (Bueter et al., 2009). When misfolded proteins accumulate in ER, protein translation increases, Ca^{2+} homeostasis is altered, as well other functions of ER will be affected thus resulting in the onset of ER stress. Under stress conditions like hypoxia, oxidative stress or heat shock, specific signaling pathways are activated that are known as unfolded protein response (UPR).

For the cells to overcome the stress condition they will activate a defense mechanism to repair the improper folded proteins, inhibit the synthesis of new proteins, and increase ER chaperone levels to resume the normal function of the cell (Sambrooks et al., 2012). Through the UPR signaling pathways, cells are induced to produce pro-apoptotic proteins and generate granules known as stress granules (Sambrooks et al., 2012). If ER stress persist, cells will be triggered to undergo apoptosis, however, in case of cancer, cells will resist apoptosis and tumor will form (Carpio et al., 2010). Under the stress conditions, Ca^{2+} is lacking and CRT acts as one of the pro-apoptotic proteins in its argynilated form (Ozcan & Tabas, 2012). CRT is argynilated through arginyl-tRNA

protein transferase (ATE) as part of UPR in which it is recruited by stress granules to activate apoptosis (Jeffery et al., 2011). Recent study has shown that ER stress induced apoptosis or ER stress is involved in different types of diseases such as cancer, neurodegeneration, type 2 diabetes, and atherosclerosis (Ozcan & Tabas, 2012).

2.1.3.5 Role of ER Stress in Obesity

There is a growing body of evidence indicating a link between ER stress and obesity, insulin resistance, type 2 diabetes, and fatty liver (Boden & Merali, 2011)(Sharma et al., 2008). It is widely known that excess nutrient intake is the main cause for obesity, and several recent studies have implicated ER stress as an early consequence of nutrient excess along with increased demand for protein synthesis to assist metabolism, local glucose deficiency due to insulin resistance, and decreased vascularization (Gregor & Hotamisligil, 2007a) (Achard & Laybutt, 2012)(Ozcan et al., 2004). This leads to accumulation of excess lipid in hypertrophied adipocytes, and abnormal energy changes observed in obesity may be a chronic stimuli causing ER stress (Fu et al., 2011). As mentioned in the above section, excess accumulation of unfolded protein aggregates will activate a process known as UPR in which also functions as regulator for the lipid metabolism under ER stress (Sambrooks et al., 2012)(Gregor & Hotamisligil, 2007b)

During ER stress, chaperone proteins play an important role in compensating for the correct folding of the newly synthesized proteins. Under quiescent or non-stressed conditions, a ubiquitous ER chaperone termed BiP or GRP78 acts as a master regulator of the UPR by binding to and inactivating these ER stress sensors (Basseri, et al., 2009). However, under conditions of ER stress, GRP78 dissociates from these sensors in order to interact and assist in the folding of luminal misfolded proteins thus activating UPR (Basseri, et al., 2009)(Prattes et al., 2000). Other chaperones such as disulfide isomerase (PDI), calnexin, the Hsp70, ERp29, CRT, and the peptidyl propyl isomerase family also play a role in the UPR process but the exact mechanism for each chaperone in relation to obesity is still unclear. In our preliminary data for another study in the lab we have observed a significant increase in the splicing of XBP-1 to sXBP-1 (one of the ER stress sensor pathways) suggesting the onset of ER stress upon overexpression of CRT (Lab's un-published data).

A study conducted by Basseri et al., hypothesized that during adipogenesis UPR activation would allow the cells to manage ER stress which exists due to the elevation of the protein load and lipid biosynthesis (Basseri et al., 2009). In this study, the authors showed that during differentiation of the 3T3-L1 preadipocytes, UPR pathways is activated and there were an increase in the expression of the ER chaperone GRP78 and if 3T3-L1 cells were treated with the ER stress inhibitor 4-PBA, adipogenesis was blocked (Prattes et al., 2000)(Chen et al., 2016) (Basseri et al., 2009).

Previous studies have suggested that ER stress may be activated in the subcutaneous fat of obese human due to excess nutrient intake (Boden, 2009). In these individuals, the adipose tissue has to uptake and store excess calories as fat and, hence, need to increase the synthesis of many proteins to meet this challenge. The massive expansion of the adipose tissue and the overwhelming need for increased protein synthesis could further contribute to the induction of ER stress. However, the exact mechanism and the role of ER chaperones specifically CRT in this process *in vivo* is still not clear.

2.2 Adipogensis/Angiogenesis

2.2.1 Adipose Tissue Structure and Functions

Although adipose tissue functions as a major storage site for fat, it is also involved in several physiological processes; including secretion of different angiogenic factors, expression of hormone receptors, cytokines and secretion of several adipokines (Lemoine et al., 2013). The amount of fat storage distribution throughout the body and their role in physiological processes varies among different species and adipose depots (Tchkonia et al., 2013). Adipose tissue depots can be distinguished by their architecture as Brown or White adipose tissues. They can also be categorized by their localization to abdominal, subcutaneous, etc.; and their secretion of different adipokines (Sierra-Honigmann, 1998).

Adipose tissue consists of a heterogeneous mixture of mature adipocytes surrounded by a stromal vascular cell fraction containing pre-adipocytes, pericytes, macrophages, endothelial cells, fibroblasts, progenitor and mesenchymal stem cells (Han et al., 2015). Active cells of adipocyte secrete a number of adipokines such as adiponectin, leptin and resistin that modulate cell metabolism (Cao et al., 2001). The level of

expression of adipokines correlates negatively or positively with the adipose mass. The released adipokines not only send signals to the brain and other organs for adipose tissue replenishment, and appetite regulation but also, they participate in the angiogenic process (Rupnick et al., 2002).

The two subtypes of adipose tissue, white and brown, are significantly vital. The main function of white adipose tissues is triacylglycerol (TG) storage when there is excess energy intake, then release of this energy in the form of fatty acids under the conditions of lack of energy (Miettinen et al., 2008a). However, brown adipose tissues that are rare in adult human are essential for production of body heat for newborn babies (Gregoire et al., 1998). Various studies demonstrated that an embryonic stem cell precursor produce adipocyte lineage with differentiation capacity into the mesodermal cell types of chondrocytes, osteoblasts, myocytes and adipocytes (Konieczny & Emerson, 1984). Adipoblasts belong to the adipogenic lineage, become pre-adipocytes and in a suitable environment it differentiates into mature lipid-storing and lipid-synthesizing adipocytes (Katz et al., 1999) (Figure 2.2). The new fat cells are produced from the precursor cells and continue throughout the lifespan. Adipocytes are considered as one of the few cells where their size can vary under physiological conditions (Farnier et al., 2003). Adipose tissue grows as they store excess energy intake. Adipose tissue expands in two ways, by increasing in adipocyte size (Hypertrophy) or increasing in adipocyte numbers (Hyperplasia). The phenotype of adipose tissues is influenced by the interaction of diet and genetics (Jo et al., 2009). Hypertrophic expansion of adipose tissue is often observed with increase in caloric intake such as in high fat diet. Hyperplastic growth of adipose tissues appears at early stages of development prior to hypertrophy to meet the needs of

lipid storage. As the size and number of adipose tissues varies, their molecular and physiological properties will show differences. This in turn can affect the metabolite profile in the circulation.

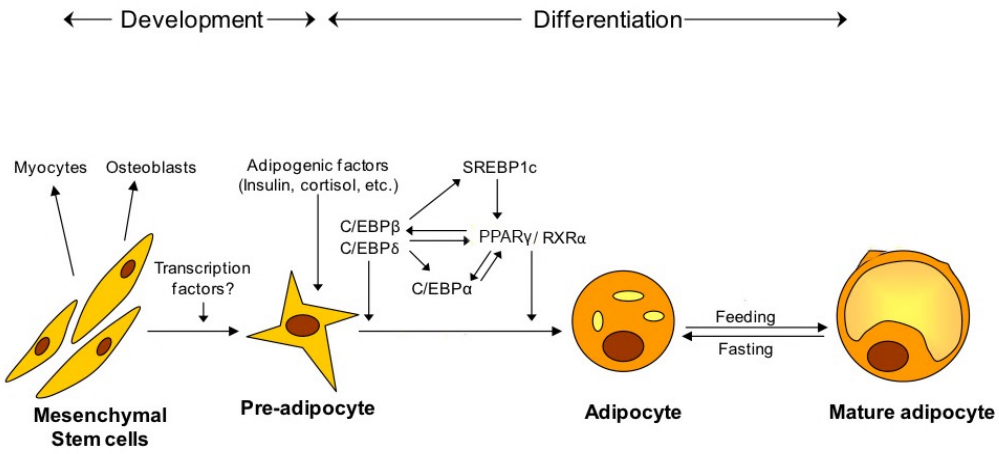

Figure 2.2 Process of adipocyte development and differentiation. In response to several transcription factors and signals, the pluripotent mesenchymal stem cells can form preadipocytes, myocytes, or osteoblasts depending upon these various promoters. Modified figure from (Garg, 2011)

2.2.2 Adipose Tissue Angiogenesis

Adipose tissue is a highly vascularized tissue (Lemoine et al., 2013) (Lijnen, 2008). The vascular networks play a vital role in the adipogenesis process. The vasculature of adipose tissue provide oxygen, growth factors, nutrients, and cytokines to the progenitor cells that are differentiated into pre-adipocytes and vascular endothelial cells (Tang et al., 2008). During embryonic development, both arteriolar differentiation and changes in extra-cellular matrix (ECM) precede differentiation of adipocytes. However, later during development of adipose tissue, throughout the whole life, it seems that adipocytes themselves drive the development and maintenance of their blood vessels (Mandrup et al., 1997). To adapt to changes in the size and metabolic rate of adipose depots, adipose vasculature requires constant regulation by several angiogenic modulators.

Adipocytes regulate angiogenesis by cell to cell contact and by adipokines secretion. For instance, adipocytes secrete pro-angiogenic growth factors like fibroblast growth factor (FGF), vascular endothelial growth factor A (VEGF-A), and leptin (Xue et al., 2009). They can also secret antiangiogenic factors including thrombospondin-1 (TSP-1), or other angiogenic modulators such as plasminogen activator inhibitor or adiponectin (Xue et al., 2009). The ratio of all these factors at any time will determine the angiogenic phenotype in the adipose tissue (Xue et al., 2009).

2.3 Endothelial Dysfunction

Vascular endothelial cells form the inner barrier of the vessel wall are responsible for maintaining the vascular vasodilation and constriction (Caballero, 2003). Endothelial dysfunction is defined as inability of the vascular endothelium layer to perform its function of regulating blood clotting and controlling relaxation of vascular wall. The cause of this dysfunction is the imbalance in the production and or release of vasodilators and vasoconstrictors affecting the narrowing and widening of the blood vessels (Lobato et al., 2012). Some of the factors responsible for the imbalance are; reduced production of nitric oxide, over-expression of adhesive molecules, over-expression of chemokines and cytokines, and an increase in the generation of reactive oxygen species in the endothelium (Kolluru et al., 2012).

Defect in the endothelial cell function has been shown to result as a consequence of different diseases such as obesity, diabetes, high blood pressure (Singhal, 2005). Studies examining this dysfunction with obesity showed that in obese people there is a direct correlation between the obesity and efficiency of endothelium vasodilators release (Lobato et al., 2012). As already mentioned, an increase or decrease in the generation of the reactive oxygen species is one of the main causes of endothelium dysfunction. These factor specifically are linking obesity to endothelial dysfunction (Adya et al., 2015).

For maintaining vascular contractility, endothelial cells generate nitric oxide through activation of endothelial nitric oxide synthase (eNOS). Altered eNOS generation could contribute to the onset of endothelial dysfunction (Montezano & Touyz, 2012). Uncoupling of eNOS is a major contributor for the generation of the reactive oxygen species that result in decreased nitric oxide (NO) bioavailability (Montezano & Touyz,

2012). The fluctuation in the balance of NO and reactive oxygen species in the endothelial cells can influence the adipocyte cells leading to the storage of fats in fat tissues and the impairment of adipocytes which may lead to obesity (Lijnen, 2008). Furthermore, decrease in NO production will influence the contractility of the vascular wall thus affecting blood flow. Previous preliminary research in Dr. Mesaeli lab on the mesenteric artery function of EC^{CRT+} mice showed a significant reduction in the relaxation of mesenteric artery in response to acetylcholine stimulation (Figure 2.3). These studies also illustrated that addition of NO donor (SNP) could recover the relaxation of the mesenteric artery of EC^{CRT+} mice (Figure 2.4) which suggest a defect in the endothelial cells on the vascular smooth muscle cells. These data suggest the onset of endothelial dysfunction upon overexpression of CRT in the endothelial cells. Based on the previous publication we suggest that endothelial dysfunction in the EC^{CRT+} mice plays an important role in the increased obesity in these mice.

Insulin resistance in endothelium layer due to endothelial dysfunction was shown to increase the formation of fat leading to obesity (Kim et al., 2006) . This hormone plays a major role in maintaining the glucose levels in the body, regulating the metabolism of proteins, lipids, and carbohydrates, thus affecting tissue development (Wilcox, 2005). Several studies have illustrated the role of insulin in vessel wall to be mediated via NO release leading to vasodilation (Potenza et al., 2005)(Montagnani et al., 2002)(Zeng et al., 2000). Vasodilation increases blood flow through the vessels leading to glucose uptake by target tissue including the skeletal muscle (Potenza et al., 2005). Insulin resistance and direct obesity correlate with dysfunction of endothelium (Prieto et al., 2014).

Diabetic patients often exhibit less supply of blood to some organs or parts of the body, because of the reduction in the angiogenic growth factors (Kolluru et al., 2011). During endothelial dysfunction, a considerable reduction in the level of NO was observed due to an increase in the superoxide anion which results in reducing the effect of angiogenic growth factors (Onat et al., 2012). A focus on the effect of NO on angiogenesis is evident in the healing of diabetic wounds (Y. Cao, 2013). Angiogenesis plays an important role in wound healing but in the case of diabetic patient wound healing is difficult due to impairment of the epithelial layer (Y. Cao, 2013)

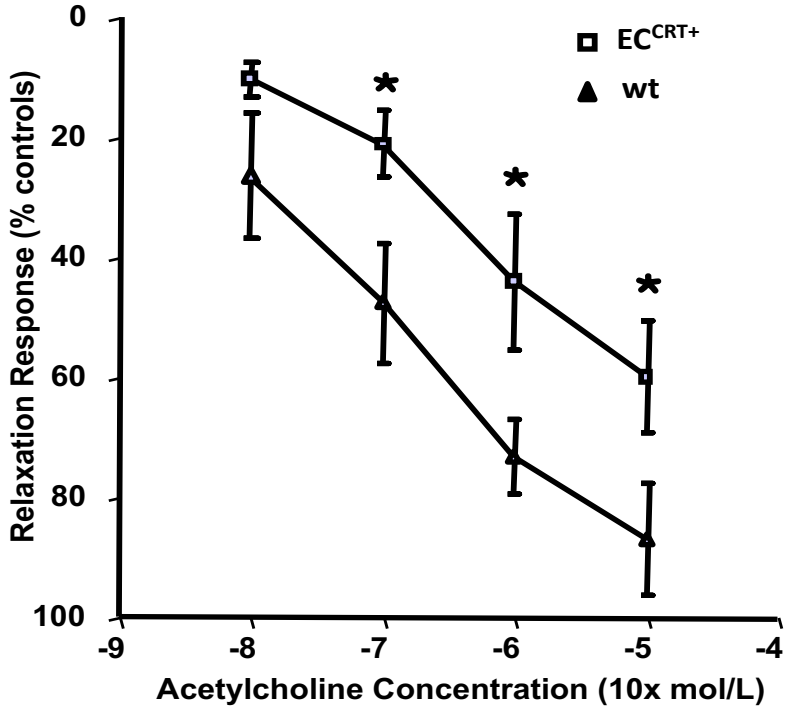

Figure 2.3 Effect of Acetylcholine on relaxation of mesenteric arteries (third branch) isolated from EC^{CRT+} as compared to *wt* mice. Data were collected from pressure myography assay. As shown there was a significantly lower relaxation of mesenteric arteries in response to acetylcholine treatment suggesting either defect in NO production or defect in smooth muscle function.

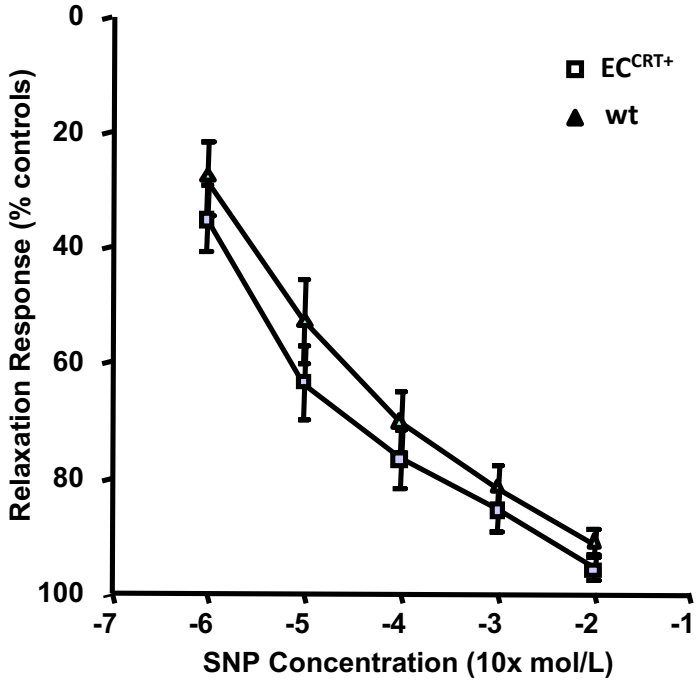

Figure 2.4 Effect of Sodium nitroprusside (SNP, NO donor) on Acetylcholine mediated relaxation of mesenteric arteries (third branch) isolated from EC^{CRT+} as compared to *wt* mice. Data were collected from pressure myography assay. As shown there was no difference in the relaxation of mesenteric arteries isolated from EC^{CRT+} mice as compared to the *wt* mice. This suggest that there is no defect in NO in smooth muscle function of these mice.

CHAPTER 3. MATERIALS AND METHODS:

3.1 MATERIALS AND REAGENTS

Material used in research included in the current thesis were of highest Molecular Biology grade and are listed in Table 3.1 to 3.6. All tables contain a list of materials/kits and their sources and their catalogue numbers (where applicable).

Table 3.1 LIST OF KITS USED IN THIS STUDY

Items	Company	Part Number
Phire Tissue Direct PCR Master Mix Kit	Thermo Fisher Scientific	F170S
Pierce™ BCA Protein Assay Kit	Thermo Fisher Scientific	23227

Table 3.2 LIST OF ANTIBODIES USED IN THIS STUDY

Items	Company	Part Number
Rabbit HA Epitope Tag	Rockland	600-401-384
Rabbit Anti-eNOS	NeoMarkers	PA1-037

Table 3.3 LIST OF REAGENTS USED IN THIS STUDY

Item	Company	Part Number
Precision Plus Protein™ Dual Color Standard	Bio-Rad	161-0374
Ponceau S Stain	Sigma	P3504-100G
DEPEX Mounting Media, Electron Microscopy Sciences	Electron Microscopy Science	100496-550
O.C.T.™ Compound	Tissue-Tek-Science Service	4583
Paraformaldehyde, Prills, 95%	Sigma	441244-3kg
Xylene	Sigma	534056-1L
Hydrochloric Acid	Sigma	25814-500mL
Absolute Ethanol	VWF	20821-321
Eosin Y di-sodium	Sigma	E4382-100G
Hematoxylin	Sigma	H9627-25G
Dulbecco's phosphate-buffered saline (DPBS)-1XPBS	Thermo Fisher Scientific	14190136
Non-Fat Skim Milk	Regilait	
Tween®20	Sigma	P9416-100mL
SuperScript™ II Reverse Transcriptase	Thermo Fisher Scientific	18064014
RNaseOUT™ Recombinant Ribonuclease Inhibitor	Thermo Fisher Scientific	10777019
Oligo(dT)12-18 Primer	Thermo Fisher Scientific	18418012
ProLong™ Gold Antifade Mountant with DAPI	Thermo Fisher Scientific	P36935
Power SYBR® Green PCR Master Mix	Thermo Fisher Scientific	4388869

Table 3.4 LIST OF INUSTRUMENT USED IN THIS STUDY

Items	Company	Part Number
Axiovision ZEISS Microscopy	Carl ZEISS Microscopy	490035-0041-000
Tissue Processer Cryostat-Frozen LEICA CM 3050S	LEICA	14047033518
Tissue Processer Microtome-Paraffin LEICA RM 2255	LEICA	1492255UL01
Licor odyssey CLX-Infrared	Licor Biotechnology	926-75001
Glucose measurement machine	One Touch Ultra-soft	Y197004
Confocal Axiovision ZEISS Microscopy	Carl ZEISS Microscopy	

Table 3.5 LIST OF SOFTWARE USED IN THIS STUDY

Items	Company
LI-COR® Image Studio™ Lite Software	Licor Biotechnology
Axiovision Software SE64 Rel.4.8.2	Carl ZEISS Microscopy
ZEN Microscope Software	Carl ZEISS Microscopy

Table 3.6 LIST OF LAB SUPPLIES USED IN THIS STUDY

Items	Company	Part Number
Disposable Base Molds	Thermo Fisher Scientific	41740
Superfrost ®Plus Micro Slide	VWF	48311-703
96 Well Clear Flat Bottom TC-Treated Culture Microplate	FALCON	353027
Nitrocellulose membrane	Life Science	66485
0.5 ml individual PCR tubes with attached flat caps	USA Scientific	1615-5510
TipOne® 0.1-10 µl Filter Pipet Tips	USA Scientific	1121-3810
TipOne®1-20 µl Beveled Filter Pipet Tips	USA Scientific	1120-1810
TipOne®1-200 µl Graduated Filter Pipet	USA Scientific	1120-8810
TipOne® 101-1000 µl Filter Pipet Tips	USA Scientific	1126-7810
Blood EDTA Tubes 1.3ml K3E	Sarstedt	41.1395.105
Glucose Strips	One Touch Ultra-soft	2730-055
MicroAmp™ Fast Optical 96-Well Reaction Plate with Barcode, 0.1 mL	Thermo Fisher Scientific	4346906

3.2 METHODS

3.2.1 Ethical approval

This study included animal samples, so the ethical approval has been obtained from the Institutional Animal Care and Use Committee (IACUC) in Weill Cornell Medicine in Qatar (WCM-Q).

3.2.2 Generation of mice model (EC^{CRT+}) - Tie2-CRT transgenic mice

The main mouse model used in my study was overexpressing CRT in endothelial cells and was developed in Dr. Mesaeli's lab in Canada. To direct CRT expression to endothelial cell, Tie2 promoter which is an endothelial specific promotor was used. CRT cDNA was cloned sandwiched between the Tie2 promoter and Tie2 enhancer as shown in (Figure 3.1). To differentiate between the exogenous and endogenous CRT, hemagglutinin tag (HA-tag) was cloned at the C-terminus of the CRT cDNA upstream of the KDEL ER retention signal sequence in CRT cDNA. Previous research in the lab showed that this cDNA of CRT has the same localization as endogenous CRT and was able to reinstitute CRT function in CRT knockout cell line, therefore it was functioning correctly. The plasmid was then digested and purified using gel extraction. The transgene was then injected into the *wt* oocytes, as a result, eight different lines of EC^{CRT+} were generated and their genotyping was confirmed by PCR. Each line was from a separate oocyte injection. The phenotype of these mice was examined overtime and they showed very similar phenotype.

3.2.3 Generation of mice model (*Cdh-EC^{CRT+}-EGFP*) transgenic mice

To examine the changes of angiogenesis in *EC^{CRT+}* mice *in vivo*, we generated a mouse line which overexpressed CRT and EGFP in the endothelial cells. To label all the endothelial cells with EGFP, we purchased *Cdh-Cre* and *B6.129(Cg)-Gt(ROSA)26Sor$^{tm4(ACTB-tdTomato,-EGFP)Luo}$/J* (ROSA-EGFP for short) mice from Jackson Laboratories USA. *ROSA-EGFP* mice express *Flox-Stop-EGFP* caste and can be used to label different cells in live mice with EGFP when they are crossed with a specific *Cre* mice. We bred these with *Cdh-Cre* at our Vivarium core at WCM-Q. This resulted in the generation of mice *Cdh-EGFP* mice in which *Cre* is activated in endothelial cells and thus excising Floxed STOP signal from EGFP leading to expression of EGFP in the endothelial cells only. The *Cdh-EGFP* mice were then bred with *EC^{CRT+}* mice to generate the *Cdh-EC^{CRT+}-EGFP* mice. These crossbred mice will express EGFP and overexpress CRT in the endothelial cells. Tissue were collected from the *Cdh- EC^{CRT+}-EGFP* mice and *Cdh-EGFP* mice (control mice) for examining *in vivo* angiogenesis. Tissue was then fixed and processed for cryo-sections as described below. The fluorescent signal in the vasculature of mice was captured by confocal microscopy. The comparison of the experimental and *wt* will be easier and less time consuming than using the other immunohistochemical techniques.

3.2.4 Genotyping of the wild-type and transgenic mice (*wt*, EC^{CRT+}, and $Cdh\text{-}EC^{CRT+}$-*EGFP*)

3.2.4.1 Polymerase chain reaction (PCR) analysis

To confirm the genotype of EC^{CRT+} transgenic mice, *Cdh-EGFP* and $Cdh\text{-}EC^{CRT+}$-*EGFP*, we used a phire tissue direct PCR master mix kit (Thermo-Scientific) following the manufacture protocol. Briefly, tip of the mouse tail was clipped using a sharp blade from different mice and placed in a mixture of dilution buffer and DNA Release provided in the kit. Samples were incubated for 5 minutes at room temperature then were preheated using heat block for 10 minutes. The samples were then centrifuged, and the supernatant was collected. A total of 1μL of the genomic DNA isolated from the tail was used for 20μL PCR reaction. We used gene specific primers for CRT-HA, Cdh, and EGFP in the PCR mixture to examine the expression of CRT cDNA-HA tag coding sequence, Cadherin and EGFP respectively. The sequences for each primer are listed in (Table 3.7). The optimum annealing temperature was determined as being 60°C. The DNA was amplified by a single denaturing cycle for one minutes at 98°C followed by 40 amplification cycles as follows: 98°C for 5 sec; 60°C for 5sec and 72°C for 20 sec. Each PCR reaction also contained a PCR positive control and negative control. PCR products were separated on a 1% agarose gel and visualized by ethidium bromide staining. Images were visualized using the Bio-Rad Gel-Doc system. A fragment with the expected band size was amplified from the transgene and was only detected in samples from transgenic mice.

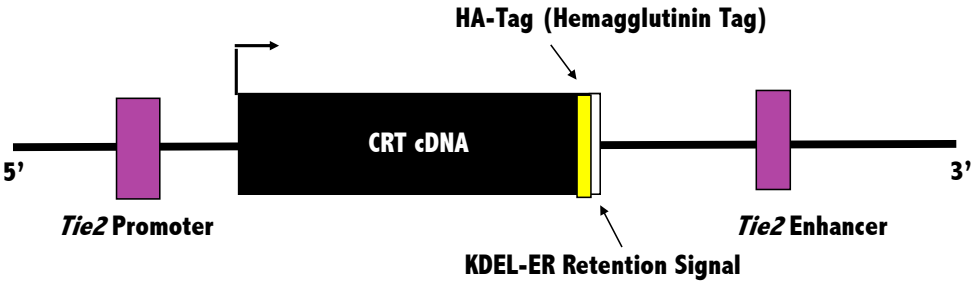

Figure 3.1 Schematic diagram showing the transgene used to generate *EC*$^{CRT+}$ mice. The transgene cassette consists of the full-length CRT cDNA including the NH2-terminal signal sequence, CRT cDNA followed by the HA epitope tag and ending with the KDEL ER retrieval signal at the COOH-terminal. The transgene was under the control of the Tie2 promoter and the Tie2 Enhancer. I would like to acknowledge Dr. Nasrin Mesaeli for designing, generating and establishing the mice colonies, genotyping and initial histo-pathological analysis of the mice in her lab in Canada.

3.2.5 Western blot analysis

The expression of different proteins in *wt* and EC^{CRT+} were determined using western blot analysis. Briefly, tissues were collected from *wt* and EC^{CRT+} and washed in ice cold phosphate buffer saline (1XPBS). Lysis buffer was added to the collected tissues for homogenization. Tissue lysates were then centrifuged at 10,000 rcf for 10 mins at 4°C. Supernatants were collected and protein concentrations were measured using Pierce™ BCA Protein Assay Kit (Thermo-scientific). A total of 40µg of the total protein for each sample was loaded on 10% SDS- polyacrylamide gel (SDS-PAGE). Protein standard Precision Plus-Protein™ Dual Color Standard (Bio-Rad) was used as a reference molecular size of the proteins. The proteins were then transferred to nitrocellulose membrane using semi-dry transfer technique.

To ensure that the proteins has been transferred completely, nitrocellulose membrane was stained with Ponceau S staining solution (Sigma) prepared in acetic acid. The nitrocellulose membrane was incubated in 5% non-fat skim milk powder prepared in 1XPBS for 60 mins at room temperature to block non-specific binding. Then, the membrane was incubated with the primary anti-body diluted in 5% non-fat skim milk in 1XPBS with continuous shaking for different time as required for each anti-body. The membrane was washed two times for 15 mins with 1XPBS containing 0.1% Tween and once with 1XPBS to remove unbinding unbound residues. The membrane was then incubated for one hour at room temperature with fluorescently tagged secondary anti-body prepared in 5% non-fat skim milk powder in 1XPBS with (1:15,000 dilution). The membrane was washed again for three times as above and visualized using Licor odyssey

CLX-Infrared (Imaging System). To ensure the equal loading of the protein samples, the same membrane was re-incubated with α-actin or Tubulin anti-body (sigma) repeating same conditions as described above.

3.2.6 Examining the endothelial dysfunction

3.2.6.1 Examining eNOS expression

Western blot analysis was carried out with proteins isolated from *wt* and EC^{CRT+} whole mesenteric arteries using a rabbit anti-eNOS (NeoMarkers) to detect the expression of enzyme nitric oxide synthase (eNOS). Further details of the western blot analyses carried out in this study are explained in section 3.2.5.

3.2.6.2 RNA extraction and quantitative real-time polymerase chain reaction (qRT-PCR) analysis

To examine changes in eNOS mRNA in the endothelium of the *wt* and EC^{CRT+} mice qRT-PCR was used. Total RNA was extracted using Trizol reagent and following manufacturer's protocol. Briefly, mesenteric artery, descending aorta and fat from mice were collected in RNAase free tubes containing 1ml Trizol reagent. A total of 200µl of chloroform per 1ml of Trizol were added to the samples. Followed by centrifugation at 13,000 rcf for 20 minutes at 4°C. Following the centrifugation, the mixture separates into three layers, lower red, phenol-chloroform phase, an interphase, and a colorless upper aqueous phase. The aqueous colorless phase where RNA remains in was transferred carefully without disturbing the interphase into fresh tube. Precipitating the RNA was done by adding 500µl isopropyl alcohol to the colorless liquid in the fresh tube. Then, mixing

and centrifugation was done at 4°C for one hour at 13,000 rcf. RNA will precipitate as small pellet on the tube side. The supernatant was removed and 750µl 75% of ethanol prepared in DEPC water were added to the samples. The samples were then centrifuged at 4°C for 10 minutes at 7500 rcf, ethanol was completely removed, and RNA pellet were dried and then dissolved in DEPC water according to the pellet size.

The cDNA was synthesized using cDNA synthesis kit (Invitrogen) following the manufacturer's instructions. A total of 25ng of the cDNA was used for qRT-PCR in a Quat Studio 6Flex thermal cycler (Applied Biosystems) using SYBR green from Invitrogen. Briefly, a total of 5µl of cDNA in a final volume of 20µl reactions were carried out in MicroAmp1 Fast Optical 96-well plates (Thermo Fischer Scientific), under the following program: 20 min at 95 C, followed by 40 cycles of 3sec at 95°C and 30sec at 60°C, and a dissociation curve. Total of 250ng of gene specific primers was used to amplify eNOS and r18S (ribosomal RNA), the list of primers is provided in (Table 3.7). eNOS target gene expression was normalized to an endogenous control (r18S) and the average Ct value from each triplicate was used to calculate fold induction of the gene in the EC^{CRT+} mice compared to the *wt* mice.

Table 3.7 LIST OF PRIMERS

Items	Forward	Reversed
CRT-HA	5’CTCATCACCAACGATGAGG3’	5’CCTGTCTAGCATAGTCAGG3’
PPARγ2	5’AAGAGCTGACCCAATGGTTG3’	5’ACCCTTGCATCCTTCACAAG3’
CEBPα	5’CAAGAACAGCAACGAGTACCG3’	5’GTCACTGGTCAACTCCAGCAC3'
ADIPOQ	5’TGTTCCTCTTAATCCTGCCCA3’	5’CCAACCTGCACAAGTTCCCTT3’
r18S	5’GTAACCCGTTGAACCCCATT3’	5’CCATCCAATCGGTAGTAGCG3’
eNOS	5’TCAGCCATCACAGTGTTCCC3’	5’ATAGCCCGCATAGCGTATCAG3’
Cdh	5’CCAGGCTGACCAAGCTGAG3’	5’CCTGGCGATCCCTGAACA3’
EGFP	5’TAGAGCTTGCGGAACCCTTC3’	5’CTTTAAGCCTGCCCAGAAGA3’

3.2.7 Characterization of the *wt* and EC^{CRT+}

3.2.7.1 Histological analysis

3.2.7.1.1 Tissue preparation

Adipose tissues were collected from the *wt* and EC^{CRT+} mice. The tissues were fixed in 4% paraformaldehyde (PFA) (paraformaldehyde, Prills, 95%-Sigma) for overnight and embedded in paraffin and processed using tissue processer machine (Fisher Tissue Path, Fisher Health care). Tissues were sectioned (5μm) using Microtome and mounted on Superfrost Plus slides (VWF, USA). The sections were placed on a heat block at 50°C overnight to adhere the section to the glass slide, then cooled at room temperature and stored until use.

3.2.7.1.2 Hematoxylin and eosin staining

Adipose tissue sections from each *wt* and EC^{CRT+} mice were stained using histological techniques to examine the phenotypic changes (shape and size) of adipocyte in these mice. Sections were stained with Hematoxylin and Eosin staining protocol of Harris Hematoxylin (Prophet et al. 1994). Briefly, sections were deparaffinized in xylene for 5 minutes followed by hydration process through serial incubation in 100, 95, and 70 % ethanol for 1 minutes each. Slides were then washed with tap water then with distilled water for total hydration. Sections were then stained with hematoxylin staining for 30 seconds (nuclear staining) and washed in running tap water for 1 minute followed by quick wash with distilled water and then differentiated in 1% acid alcohol (1% hydrochloric acid in 70% ethanol) for 30 seconds.

Slides were washed in running tap water for 1 minute and counterstained in eosin-phloxine solution (quick – 7 dunks) for cytoplasmic staining. After staining, sections were washed and dehydrated through two changes of 95% alcohol and absolute alcohol for 2 minutes for each, then cleared in xylene for 5 minutes twice. Coverslips were then mounted on slides with pre-mount mounting media (Electron microscopy science).

3.2.7.1.3 Quantification of adipocyte size and numbers

5-6 images were obtained from each section of adipose tissue isolated from the *wt* and EC^{CRT} fed standard diet. Tissues were analyzed to quantify the size and number of adipocytes in each field using a Zeiss Axiovision microscope equipped with an AxioCam and analyzed with the Axiovision SE64 version 4.8 program. Adipocytes at the image borders were calculated as a number by drawing a line inside the adipocyte, but they were not counted for size quantification. as shown in (Figure 3.2)

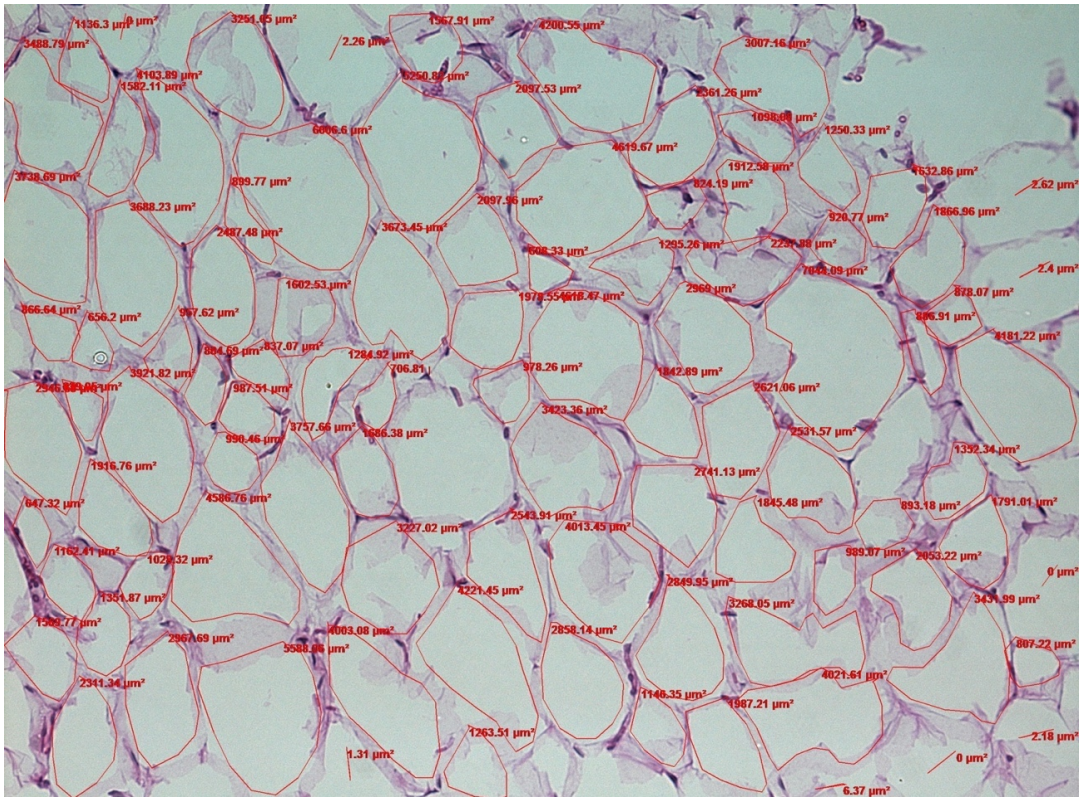

Figure 3.2 Quantification of the adipocyte size and number. By using Axiovision SE64 software the quantification has been done by drawing on the adipocyte as shown in the figure which gave the size of the adipocyte and represent the numbers. Adipocytes at the figure borders were calculated as a number by drawing a line inside the adipocyte, but they were not counted for size quantification.

3.2.8 Diet experiment of the *wt* and EC^{CRT+} mice

To examine the effect of diet on the phenotype of the *wt* and EC^{CRT+}, 4 weeks old *wt* and EC^{CRT+} litter-mate mice were fed with special diet containing either high fat (60%) or regular fat (10%) diet for different length (8-24 weeks). 20 pellets of food which is equal to 20 grams of food per week was given to these mice. A total of 10 mice was included in each group. Body weight and blood glucose measurements using one touch ultra-soft machine were obtained for each mouse bi-weekly after fasting the mice for 6 hours. At the end time of study for each group, glucose tolerance test (GTT) were measured for each mouse (see details below). The next day after the GTT test, mice were euthanized; blood, epididymal fat, liver, descending aorta, kidney, heart, lungs, and skeletal muscle were collected. Fat tissues were sectioned and stained using histological techniques for quantification of the adipocytes size and number. Phenotypic characteristics that observed visually were also recorded. Serum was collected and used for metabolomics analysis by Metabolon LTD, USA.

3.2.8.1 Glucose tolerance test (GTT)

At the end time point, each mouse fed the high fat (60%) or regular fat (10%) diet was fasted for 16 hours then body weight was measured, and 2g glucose/kg body weight of sterilized glucose was injected intraperitoneally into the mice according to their body weight. Blood samples was collected every 30 minutes up to 2 hours to check the glucose level in mg/dl.

3.2.8.2 RNA extraction and quantitative real-time polymerase chain reaction (qRT-PCR) analysis

Fat tissues were isolated from the *wt* and EC^{CRT+} mice of different group (8w, 16w, and 24w) to examine the changes in gene expression of the most studied genes related to adipogensis (Adiponectin, PPARγ, and CEBPα). Further details for RNA extraction and qRT-PCR analysis carried out in this study are explained in section 3.2.6.2.

3.2.9 Angiogenesis in *Cdh-EC^{CRT+}-EGFP*

To examine changes in angiogenesis in the transgenic mice, heart, fat, descending aorta and mesenteric artery tissues were collected from the *Cdh-EC^{CRT+}-EGFP* and *Cdh-EGFP* mice and fixed in 4% PFA and then was proceed for histological sectioning as previously described in section [3.2.7.1.1 Tissue preparation]. Images were taken using a Zeiss Confocal microscope.

3.2.10 Statistical analysis

The data was analyzed using widely accepted statistical software (Prism). Unpaired student's T-test was used for adipocyte quantification and ANOVA was used for GTT analysis. Significant difference was defined as P value<0.05. For qRT-PCR analysis, results were calculated using the ΔΔCT and are expressed as the mean ±S.D. of three samples each assayed in duplicate.

CHAPTER 4. RESULT

4.1 Genotyping confirmation of the wild-type and transgenic mice (*wt*, EC^{CRT+}, and *Cdh-*EC^{CRT+}*-EGFP*)

Mice were generated at WCM-Q by breeding, tail biopsies from these mice were used for genotyping, by PCR and western blot, to identify the transgenic mice overexpressing CRT under the control of Tie2 promotor (EC^{CRT}) and the *wt*. Figure 4.1A shows a representative Western blot of the protein isolated from mouse tails blotted with anti-HA antibody. Figure 4.1B, shows a representative PCR image of the genomic DNA and specific primers of CRT C-terminus and HA tag (Table 3.7) demonstrating the desired band of CRT-HA amplification in the transgenic mice, EC^{CRT+}, and absence of this band in the *wt* mice. Genotyping of *Cdh-*EC^{CRT+}*-EGFP* and *Cdh- EGFP* was carried out as described in material and methods using specific primers to detect VE-Cadherin, CRT-HA and EGFP listed in (Table 3.7). Figure 4.2A, B, and C illustrates the results of a representative PCR using the three different primers to amplify the target sequence. CRT-HA positive and negative, Cdh, and EGFP positive transgenic mice which were used for examining the angiogenesis differences between these mice.

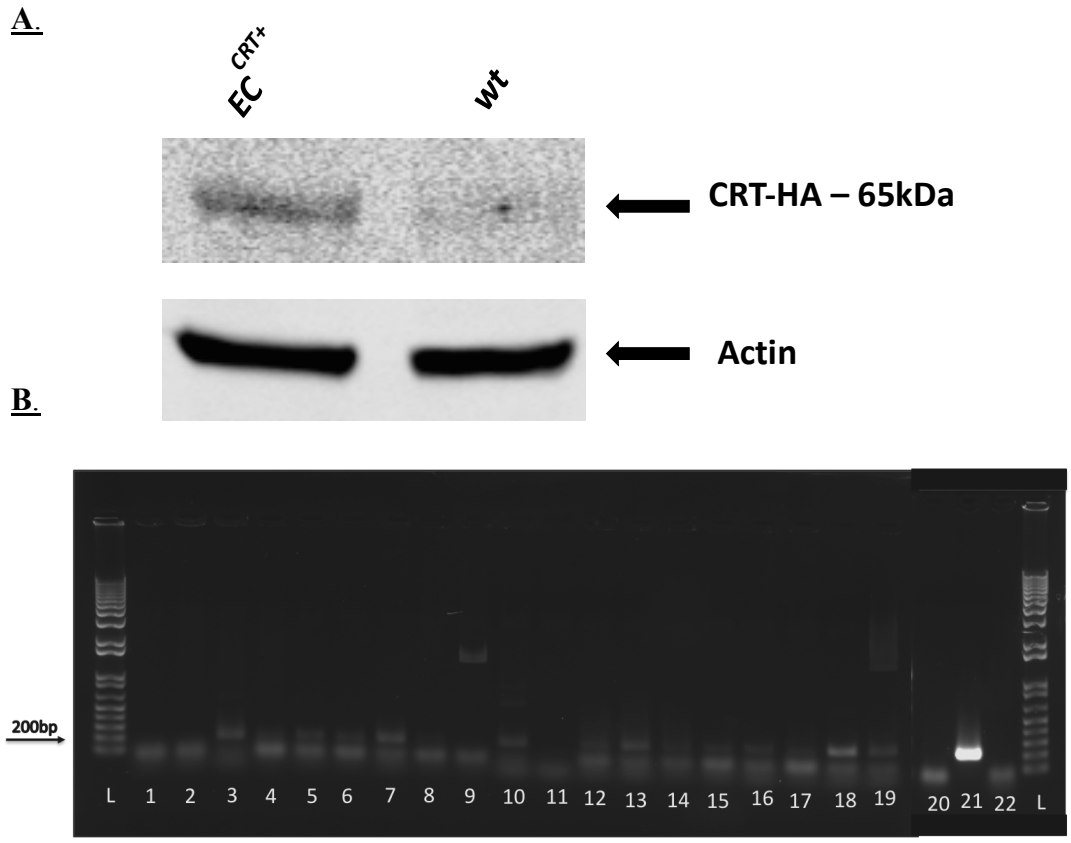

Figure 4.1 Genotyping of *EC*$^{CRT+}$ mice Transgenic mice using tail biopsies. (A) A representative Western blot analysis using an anti-HA antibody and anti-actin as a loading control. A single protein band at 65 kDa was detected in the *EC*^{CRT} samples only. (B) Using the genomic DNA isolated from tail biopsies and specific primers PCR was performed as described in Material and Methods. A representative gel shows the PCR product of genomic DNA of *EC*^{CRT} mice and *wt* A 200 bp amplicon was detected in the samples from transgenic mice only (samples: 3-7,10, 12-17, 18, 19 are positive) (samples:1, 2, 8, 9, 11, 20 are negative). Sample 21 represent the positive control and sample 22 represent the negative control where L is 1kb ladder.

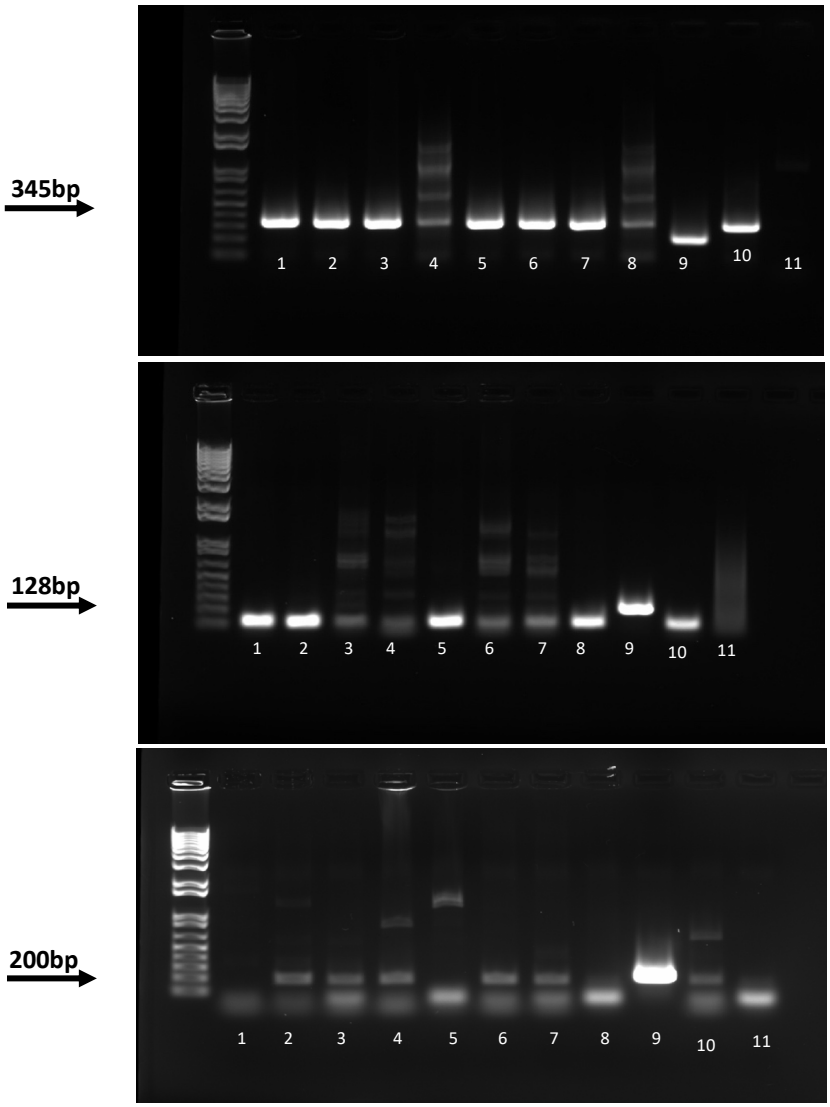

Figure 4.2 Genotyping of *Cdh-EC^{CRT+}-EGFP* and *Cdh-EGFP* by PCR analysis. PCR reaction of the genomic DNA from mouse litters were set to identify Cadherin, EGFP and CRT-HA. Samples in lane 1-8 were PCR of genomic DNA of transgenic mice lane 9 and 10 are the positive control (a universal primer and gene specific primer respectively). A) A representative PCR for *Cdh-cre*, B) A representative PCR for EGFP primer. C) A representative PCR for CRT-HA primer.

4.2 Examining the presence of endothelial dysfunction in the transgenic mice EC^{CRT+}

One of the objective of our study was to examine changes in endothelial function in the EC^{CRT+} mice. As mentioned earlier, preliminary data from our lab on the vascular function showed a significant decrease in mesenteric artery relaxation after administration of acetylcholine in the EC^{CRT+} mice compared to the *wt* mice. The defect in relaxation was overcome when applying a NO donor SNP. This observation suggested that the EC^{CRT+} mice suffer from endothelial dysfunction as a result in changes in NO production. To examine the status of eNOS in the EC^{CRT+} mice, western and qRT-PCR was carried out. Figure 4.3, illustrates that eNOS protein expression is significantly reduced in EC^{CRT+} mesenteric arteries as compared to the *wt* mesenteric arteries. In the western blot HUVEC cell (human umbilical vein endothelial cells) lysates were used as a positive control because they are expressing eNOS. As shown in the Figure 4.3, eNOS is expressed in the HUVEC, *wt* and the EC^{CRT+} mesenteric arteries. However, in the transgenic mice, the expression of eNOS is significantly decreased.

To determine whether changes observed in eNOS protein is due to gene expression or protein stability we carried out qRT-PCR of eNOS on RNA isolated from different arteries and adipose tissue from the *wt* and transgenic mice. Figures 4.4 summarizes the qRT-PCR results for the expression of eNOS gene on the isolated mesenteric artery, descending aorta and fat tissues from 4-5 different *wt* and EC^{CRT+} mice. As shown there was a significant reduction in eNOS mRNA in different tissues isolated from the EC^{CRT+} as compared to the *wt*.

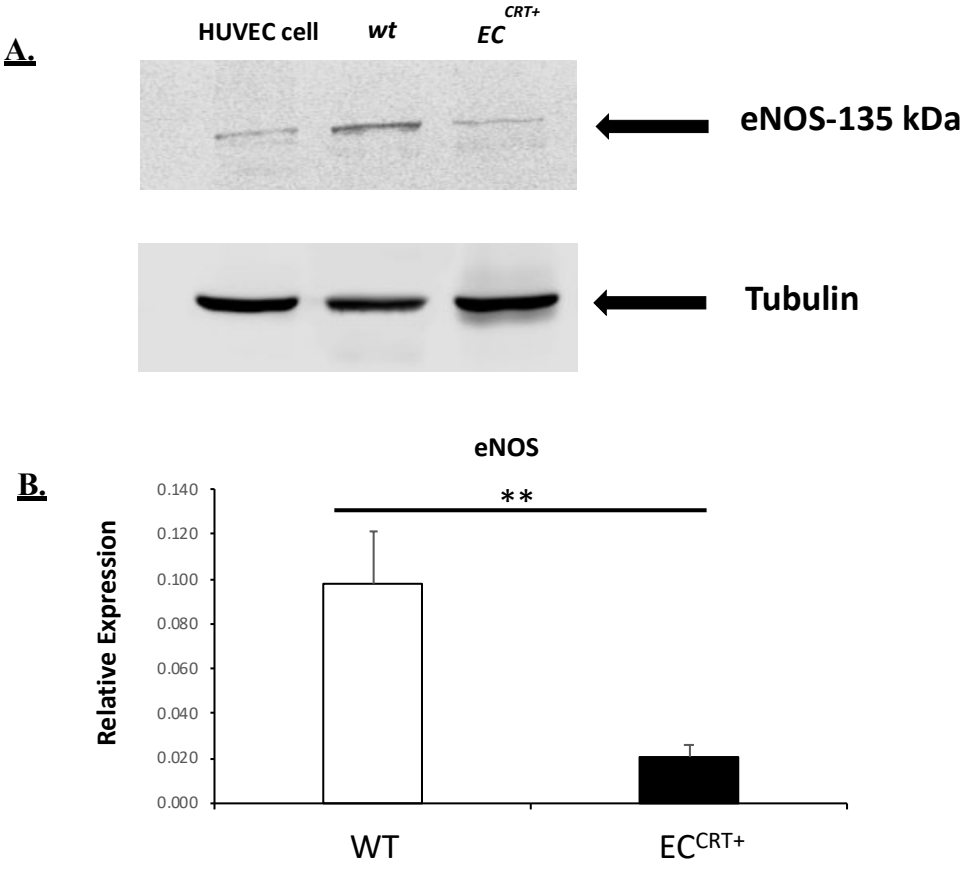

Figure 4.3 eNOS expression of *EC*$^{CRT+}$ and *wt* mice. Western blot analysis using an anti-eNOS antibody and anti-tubulin as a loading control. (A) Proteins extracted from HUVEC cell line (endothelial cells) and mesenteric arteries isolated from the *wt* and *EC*^{CRT} mice was resolved on a 7.5% SDS acrylamide gel. Lower panel is the same blot probed with antibody to Tubulin to assess equal loading of the samples. (B) eNOS protein quantification. Bar graphs are mean ± SE of n=3 mice in each group. ** P<0.01, as compared to the *wt* mice.

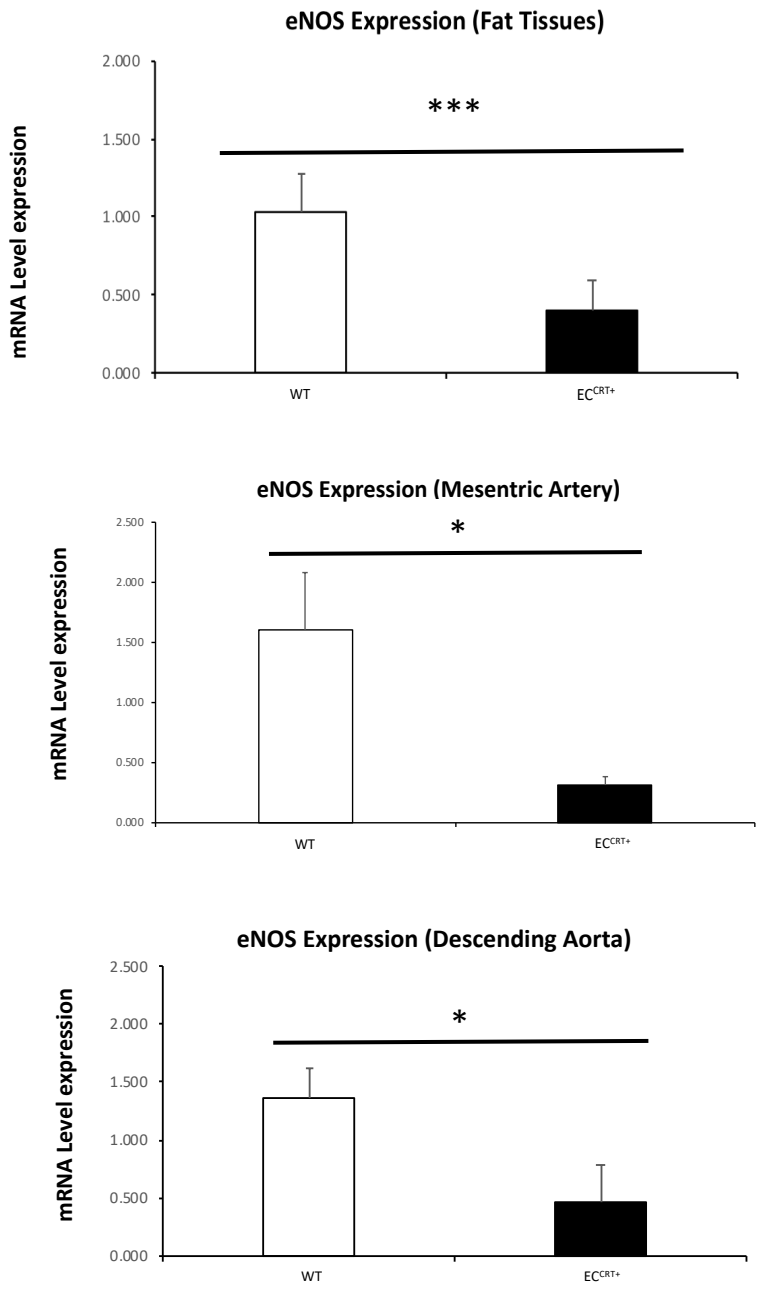

Figure 4.4 Quantification of qRT-PCR of eNOS in different tissues of *wt* and *EC^{CRT+}* mice. The qRT-PCR was carried on 4-5 separate RNA extractions. ΔΔCT was calculated to reference gene r18S for each sample. Bar graphs are mean ± SE of n=4-5 mice in each group. * P<0.05, ***P<0.001 as compared to the *wt* mice.

4.3 Characterization of adipose tissue in the EC^{CRT+} and *wt* mice

One of the phenotypes that we observed while observing the EC^{CRT+} mice as they aged was increased amount of adipose tissue, specifically in the mesenteric region and associated with different internal organs and subcutaneous area, as compared to the *wt* mice. Therefore, we aimed to characterize the adipose tissue. The epididymal fat pad was isolated from different mice and fixed and prepared for histological analysis. As shown in Figure 4.5 hematoxylin and Eosin staining, there was a significant increase in the number of adipocytes in the fat pad of EC^{CRT+} as compared to the *wt* mice. Furthermore, we observed a significant reduction in the size of the adipocytes in the EC^{CRT+} as compared to the *wt* mice (Figure 4.5). The mice we examined in this experiment were fed a normal diet. This prompted us to expand our study and examine effect of normal fat diet (10%) and high fat diet (60%) on the adipocyte phenotype in these mice.

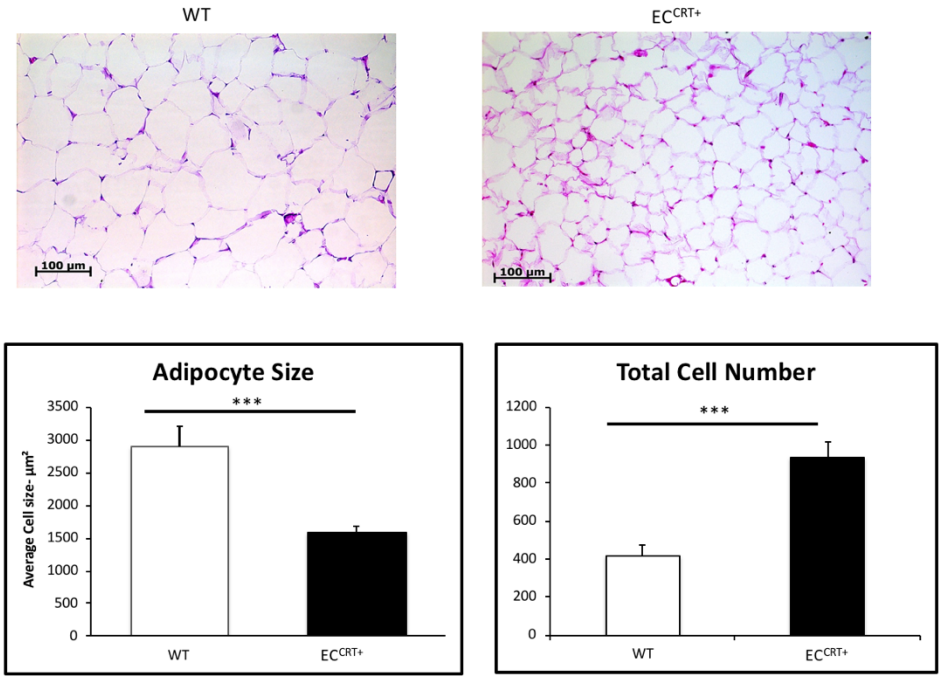

Figure 4.5 Characteristics of Adipocyte tissues. Hematoxylin and Eosin staining of epididymal adipose tissue from EC^{CRT+} and *wt* mice on standard diet. 5-6 Image field from each specimen was analyzed to quantify the number and size of adipocytes in each field. Bar graphs showing the mean ± SE of 6 separate *wt* or EC^{CRT+} mice. *** P<0.001 as compared to the *wt* mice.

4.4 Characterization of metabolic phenotype in *wt* and EC^{CRT+} mice on different diet

4.4.1 Body weight measurements

To determine effect of increased fat intake on the phenotype of the EC^{CRT+} mice we fed the mice 10% or 60 fat diet for different time periods (8, 12, 16, 20 and 24 weeks). In this report I will highlight the changes in the 8, 16 and 24 weeks. The body weight of *wt* and EC^{CRT+} mice fed for 8, 16 and 24 weeks were measured and recorded bi-weekly. At the end of time point the body weight was recorded and summarized in Figure 4.6. As seen in this figure, both the *wt* and EC^{CRT+} mice showed an increase in the body weight as the mice aged from week 8 to week 24 under 10% and 60% fat diet. Furthermore, both the *wt* and EC^{CRT+} mice body weight significantly increased after feeding mice 60% fat diet at 8 and 24 weeks as compared to the 10% fat diet. Interestingly, at 16 weeks, only EC^{CRT+} mice showed a significant increase in body weight on 60% fat diet.

4.4.2 Glucose tolerance test

As part of metabolic phenotyping of the mice we measured changes in blood glucose of the mice at end of time of treatment (8, 16 and 24 weeks). At the end of each time point *wt* and EC^{CRT+} mice fed the high fat (60%) or regular fat (10%) diet was sat for GTT. As described in materials and methods, the measurement was taken every 30 minutes for two hours. As shown in figure 4.7 there were some differences in glucose uptake in the EC^{CRT+} mice as compared to the *wt* fed 10% fat diet. The difference was significant at 24 weeks of age. However, under high fat diet, the glucose failed to return to normal level at 2 hrs. in the EC^{CRT+} mice compared to the *wt* (Figure 4.7D). At 16 and 24 weeks GTT was significantly different between the EC^{CRT+} mice and the *wt* mice under 60% fat.

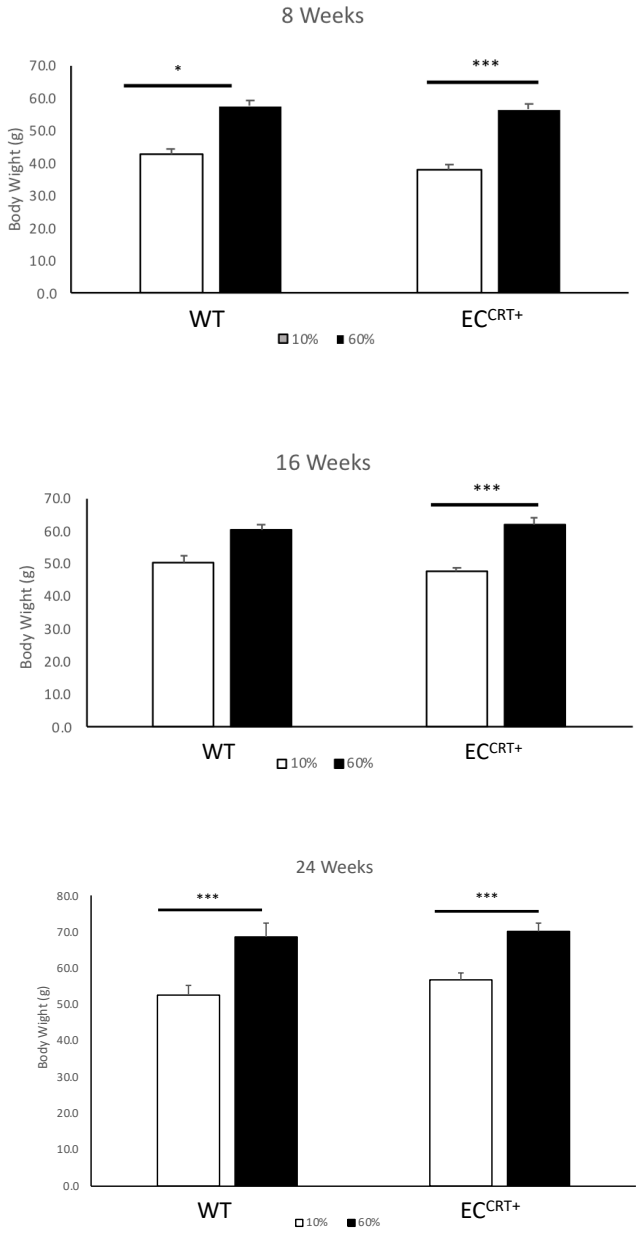

Figure 4.6 Body weight measurements of *EC^{CRT+}* and *wt* mice. Mice were fed a diet containing 10% or 60% fat for 8,16, and 24 weeks. At end of the treatment dates mice were weighed. Data were represented as bar graphs as mean ± SE of n=10 mice in each group. * P<0.05, ***P<0.001as compared to the 10% fat diet.

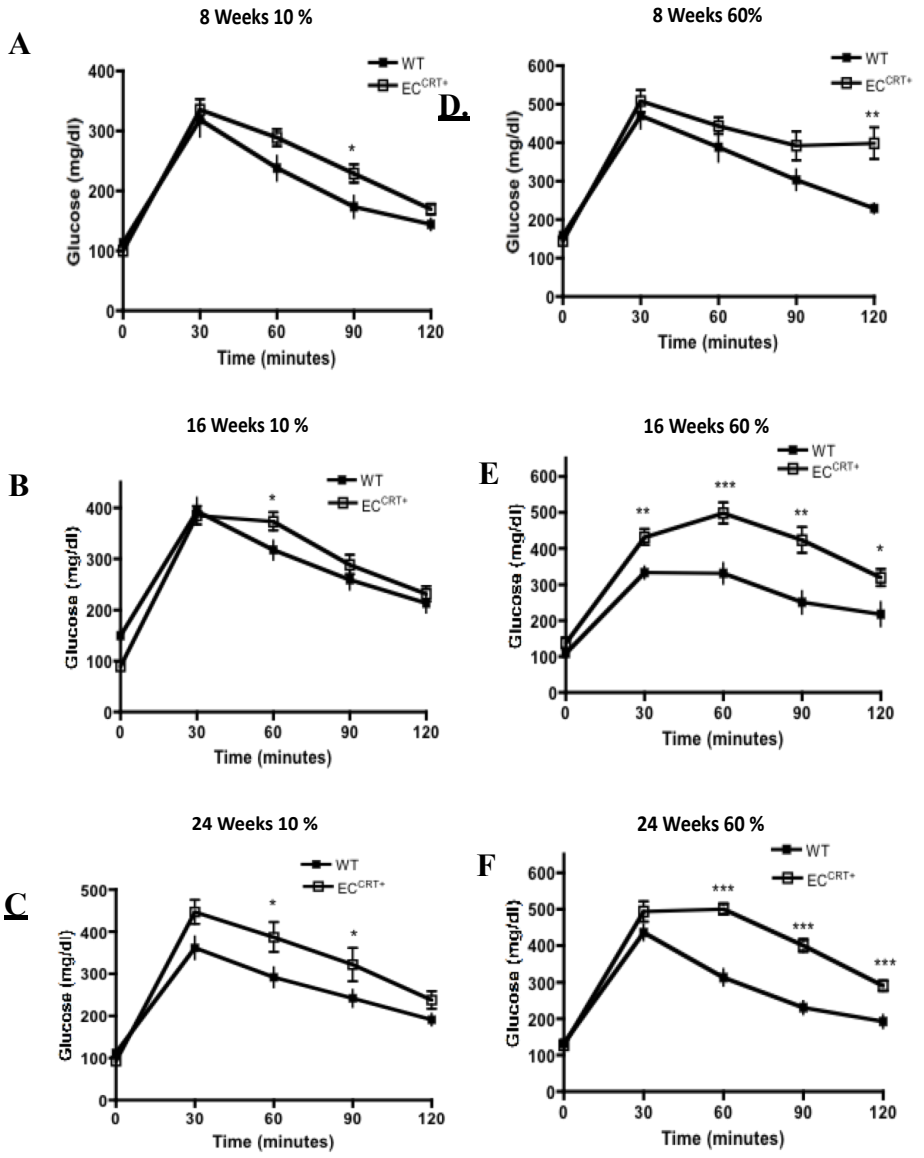

Figure 4.7 Glucose tolerance test of *wt* and *EC^{CRT+}* mice. Mice were fed a diet containing 10% or 60% fat for 8,16, and 24 weeks. At end of the treatment dates mice were weighed and glucose tolerance test was performed as described in Materials and Methods. Values were plotted against time to show the difference between the *wt* and *EC^{CRT+}* mice. Data were represented as bar graphs as mean ± SE of n=10 mice in each group. * P<0.05, ** P<0.01, ***P<0.001 as compared to the *wt* mice.

4.4.3 Phenotype of adipose tissue in *wt* and transgenic mice fed different diet

To determine effect of increased fat intake on the size and number of adipocytes of the *wt* and EC^{CRT+} mice, epididymal fat tissues were isolated from the EC^{CRT+} and *wt* mice fed normal fat (10% Fat) and high fat diet (60%) for 8, 16 and 24 weeks. As shown in figure 4.8A, the adipocyte size in EC^{CRT+} mice fed 10% fat diet for 8 weeks was significantly lower as compared to the *wt* adipocytes. Furthermore, the total number of adipocytes at 8 weeks were significantly increased in EC^{CRT+} as compared with the *wt* (Figure 4.8B). Similarly, EC^{CRT+} mice fed 10% diet for 16 weeks showed a significantly lower cell size as compared to the *wt* with no change in cell number (Figure 4.9A and B). Interestingly, mice fed 10% fat diet for 24 weeks showed a significantly higher adipocyte size (Figure 4.10A) with no change in the number of adipocytes (Figure 4.10B).

Figure 4.11 shows that when the mice were fed high fat diet (60%) for 8 weeks there were no difference in the adipocyte size and number between the two-mouse strain (EC^{CRT+} and *wt*). Similar data was observed when mice were fed 60% fat diet for 16 weeks (Figure 4.12). However, after 24 weeks on 60% diet the adipocytes in the EC^{CRT+} mice were significantly smaller as compared to the *wt* (Figure 4.12A) and they were significantly higher in number as compared to the *wt* mice (Figure 4.12B).

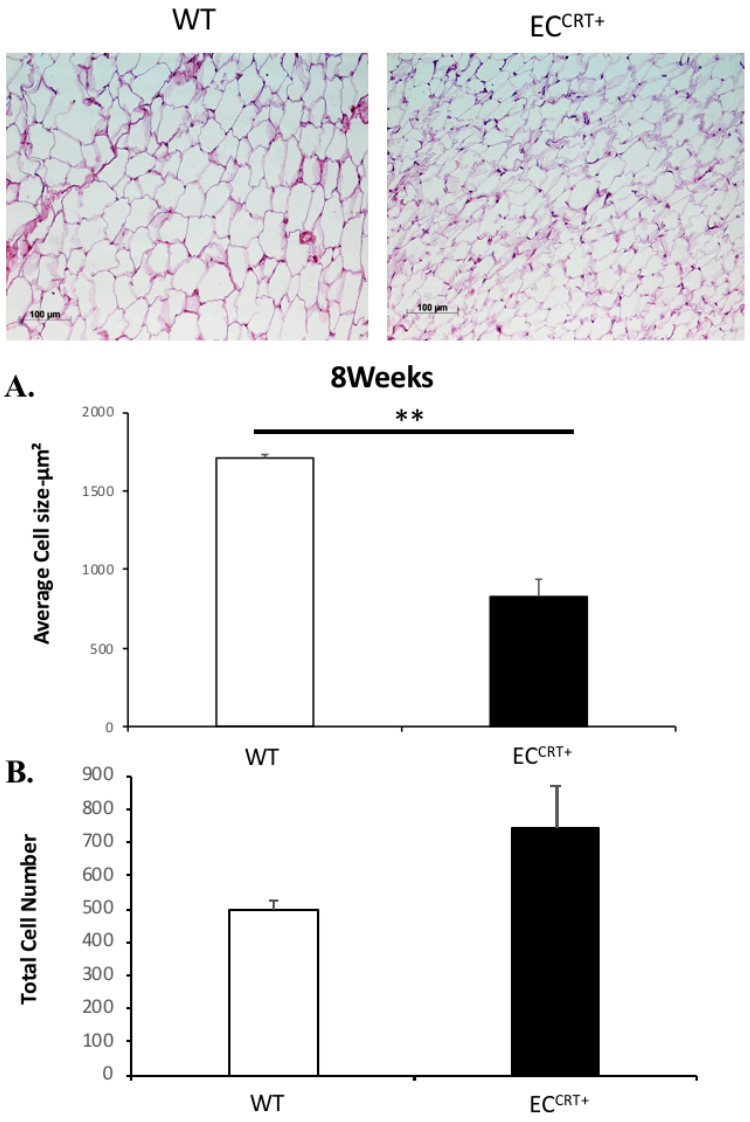

Figure 4.8 Characteristics of Adipocyte tissues isolated from mice fed <u>10% fat diet for 8 weeks</u>. Hematoxylin and Eosin staining of adipose tissue from *wt* mice and EC^{CRT+} mice on 10% fat diet. 5-6 Image fields from each specimen was analyzed to quantify the size (A) and number (B) of adipocytes in each field. Bar graphs showing the mean ± SE of 3 separate *wt* or EC^{CRT+} mice. ** P<0.01, significantly different from the *wt* mice.

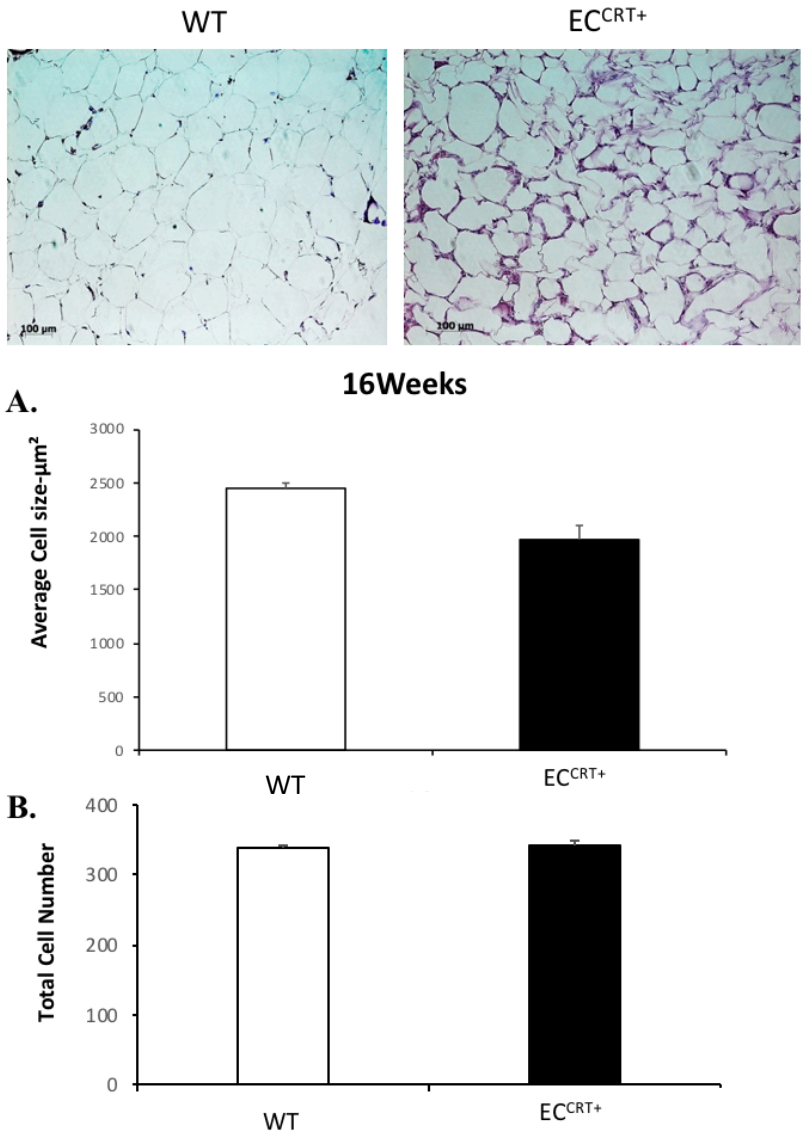

Figure 4.9 Characteristics of Adipocyte tissues isolated from mice fed <u>10% fat diet for 16 weeks</u>. Hematoxylin and Eosin staining of adipose tissue from *wt* mice and *EC*$^{CRT+}$ mice on 10% fat diet. 5-6 Image fields from each specimen was analyzed to quantify the size (A) and number (B) of adipocytes in each field. Bar graphs showing the mean ± SE of 3 separate *wt* or *EC*$^{CRT+}$ mice. No significant differences observed.

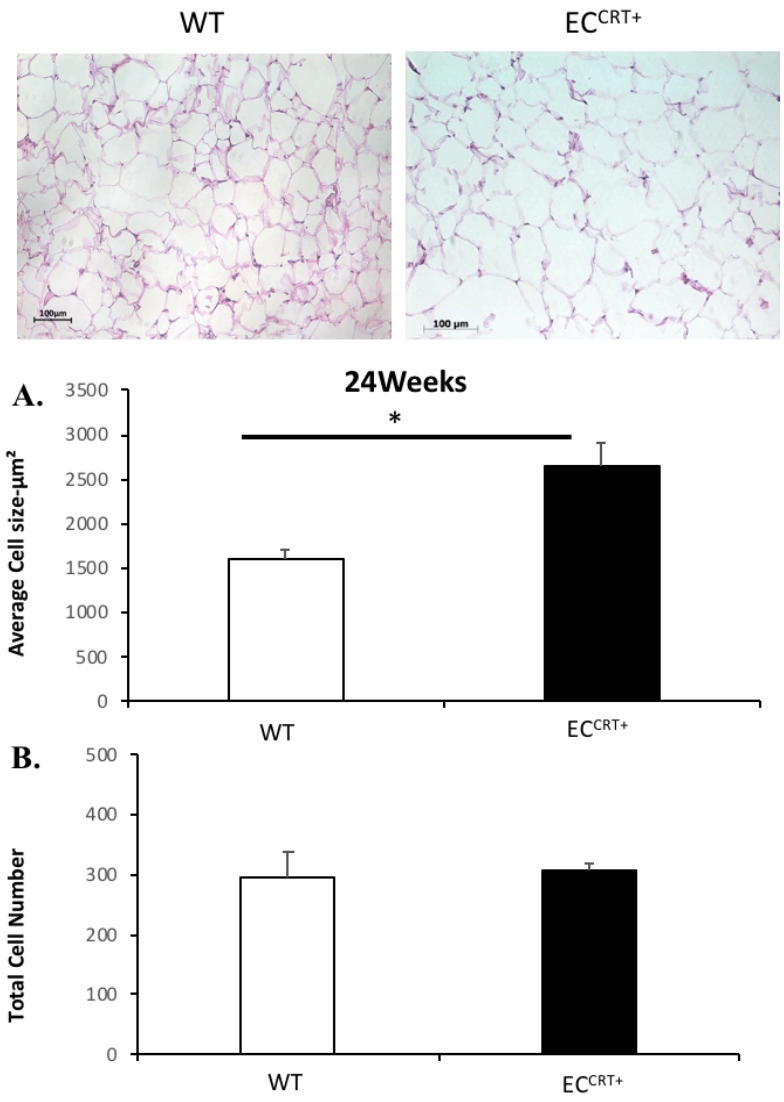

Figure 4.10 Characteristics of Adipocyte tissues isolated from mice fed <u>10% fat diet for 24 weeks.</u> Hematoxylin and Eosin staining of adipose tissue from *wt* mice and EC^{CRT+} mice on 10% fat diet. 5-6 Image fields from each specimen was analyzed to quantify the size (A) and number (B) of adipocytes in each field. Bar graphs showing the mean ± SE of 3 separate *wt* or EC^{CRT+} mice. * $P<0.05$, significantly different from the *wt* mice.

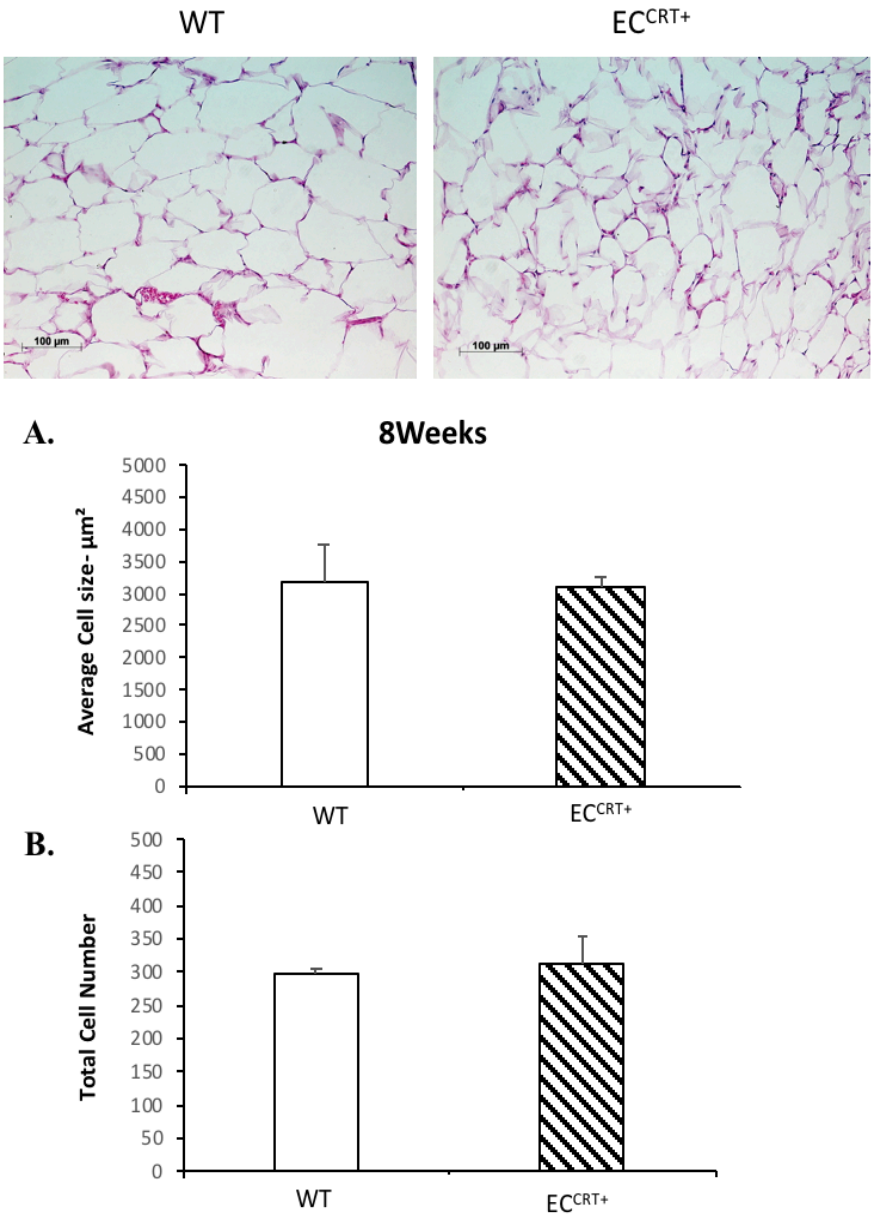

Figure 4.11 Characteristics of Adipocyte tissues isolated from mice fed <u>60% fat diet for 8 weeks</u>. Hematoxylin and Eosin staining of adipose tissue from *wt* mice and EC^{CRT+} mice on 60% fat diet. 5-6 Image fields from each specimen was analyzed to quantify the size (A) and number (B)of adipocytes in each field. Bar graphs showing the mean ± SE of 3 separate *wt* or EC^{CRT+} mice. No significant differences observed.

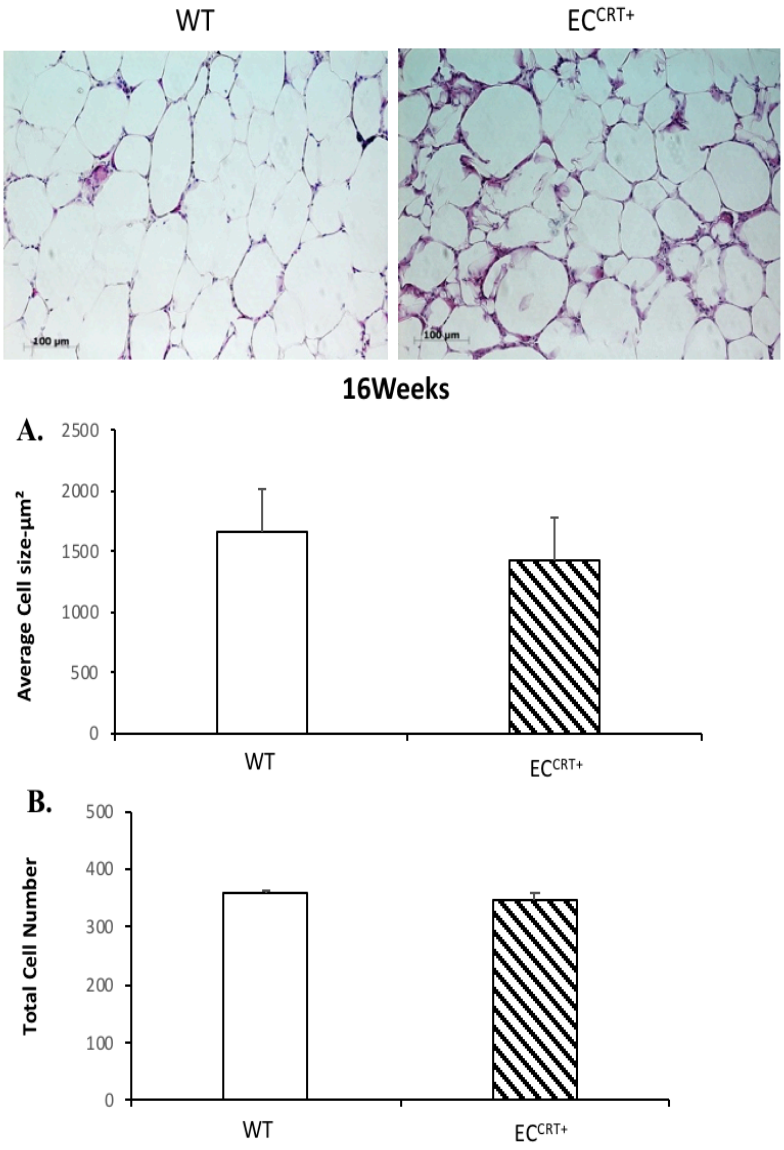

Figure 4.12 Characteristics of Adipocyte tissues isolated from mice fed <u>60% fat diet for 16 weeks</u>. Hematoxylin and Eosin staining of adipose tissue from *wt* mice and EC^{CRT+} mice on 60% fat diet. 5-6 Image fields from each specimen was analyzed to quantify the size (A) and number (B)of adipocytes in each field. Bar graphs showing the mean ± SE of 3 separate *wt* or EC^{CRT+} mice. No significant differences observed.

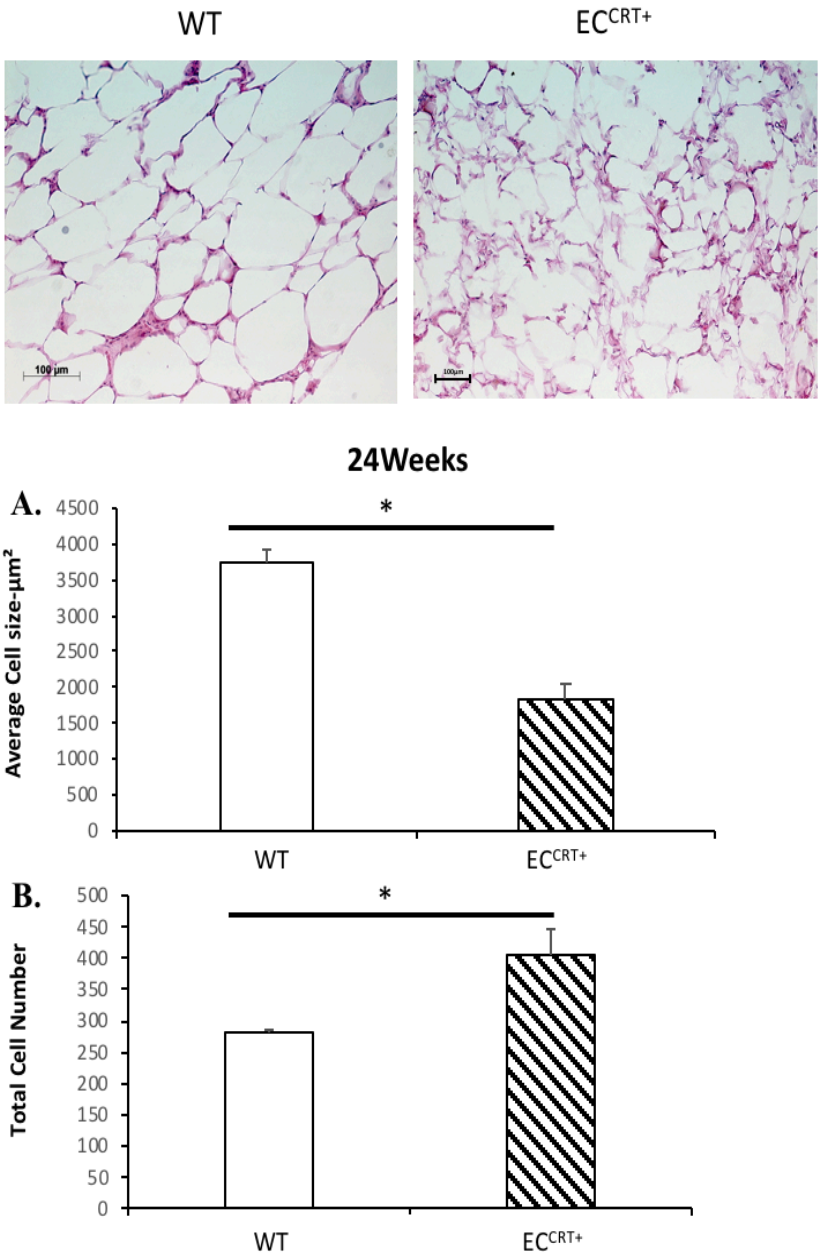

Figure 4.13 Characteristics of Adipocyte tissues isolated from mice fed 60% fat diet for 24 weeks. Hematoxylin and Eosin staining of adipose tissue from *wt* mice and *EC*$^{CRT+}$ mice on 60% fat diet. 5-6 Image fields from each specimen was analyzed to quantify the size (A) and number (B)of adipocytes in each field. Bar graphs showing the mean ± SE of 3 separate *wt* or *EC*$^{CRT+}$ mice. * P<0.05, significantly different from the *wt* mice.

4.5 Adipocyte specific gene expression profile

As shown above there was a significant change in the adipocyte phenotype of the *wt* and EC^{CRT+} epididymal fat fed different fat diet. Therefore, we examined changed in expression of some fat specific transcription factors, Adiponectin, PPARγ, CEBPα. Figures (4.14, 4.15 and 4.16) summarizes the qRT-PCR results for the expression of the three tested genes in the epididymal fat isolated from *wt* and EC^{CRT+} mice fed 10% and 60% fat diet for different times. As shown in Figure 4.14 adiponectin expression was lower in EC^{CRT+} fed with 10% fat diet as compared to the *wt* at the 3 times tested (Figure 4.14 A). Interestingly, feeding the mice with 60% diet reduced expression of adiponectin in both the *wt* and the EC^{CRT+} mice (Figure 4.14B). The variation in the standard error bar was due to the variation between the mice of the same group although they were showing the same trend of genes that is downregulated.

Figure 4.15 shows changes in the expression of PPARγ in the epididymal fat isolated from the *wt* and the EC^{CRT+} mice fed different diets. There was a significant decrease in PPARγ expression in mice fed 10% fat diet for 8 and 16 weeks with no difference in the 24 weeks time point (Figure 4.15B). However, after high fat diet (60% fat) PPARγ expression was reduced in the EC^{CRT+} mice at all the three-time points (Figure 4.15B.

Figure 4.16 summarizes the qRT-PCR data for CEBPα expression in the epididymal fat isolated from the *wt* and the EC^{CRT+} mice fed different diets. 10% fat diet had no significant difference in CEBPα expression at different weeks between the *wt* and the EC^{CRT+} mice (Figure 4.16A). Interestingly, feeding mice a diet containing 60% fat significantly reduced the expression of CEBPα in the EC^{CRT+} mice as compared to the *wt* mice at 8 and 16 weeks (Figure 4.16 B). Furthermore, at 24 weeks feeding with 60% fat diet, we observed no significant change in the CEBPα expression (Figure 4.16B).

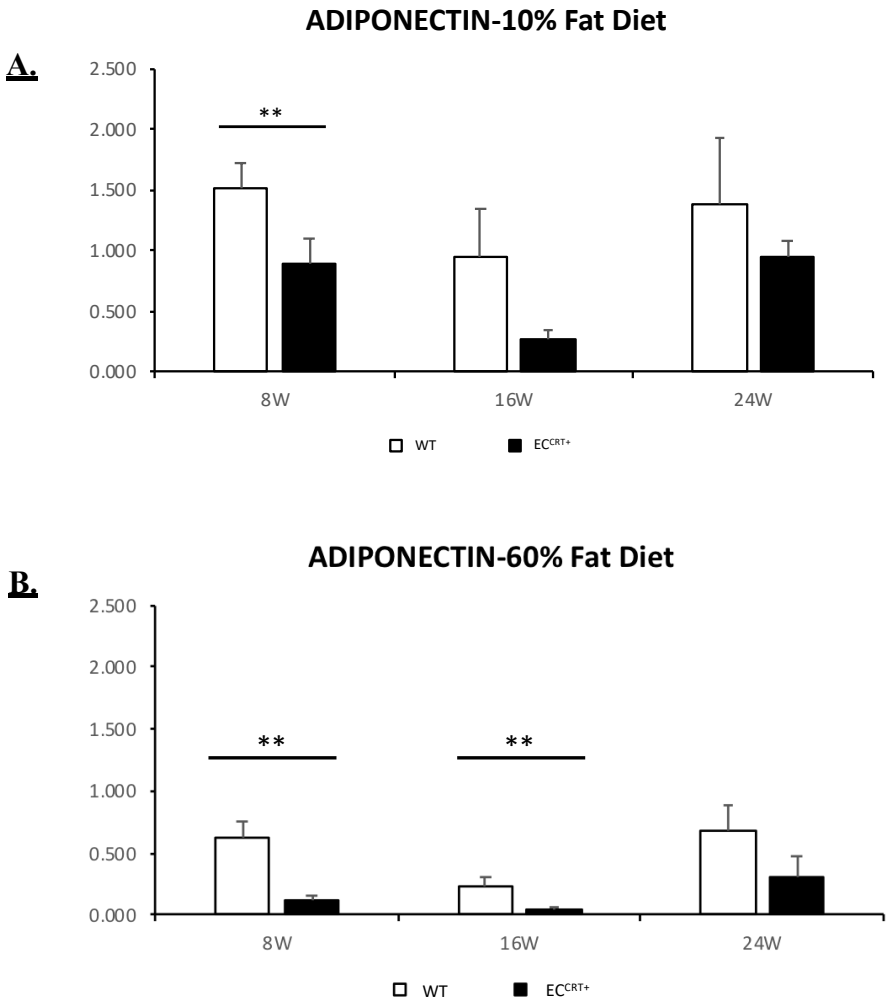

Figure 4.14 qRT-PCR of fat tissue of *EC*$^{CRT+}$ and *wt* mice under 10% and 60% fat diet. The figure shows the mRNA level of ADIPONECTIN. Downregulation of the three genes was observed on the mice under both fat diet (10% or 60%). Bar graphs are mean ± SE of n=3-6 mice in each group. ** P<0.01, as compared to the *wt* mice.

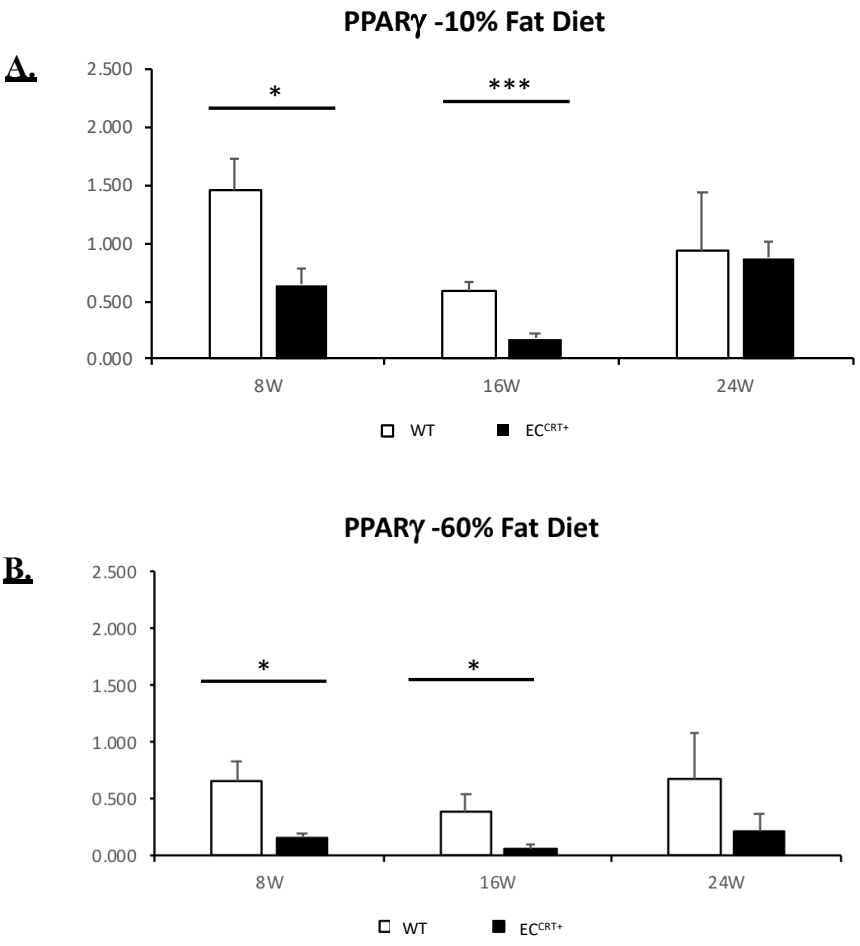

Figure 4.15 qRT-PCR of fat tissue of *EC^{CRT+}* and *wt* mice under 10% and 60% fat diet. The figure shows the mRNA level of PPARγ. Downregulation of the three genes was observed on the mice under both fat diet (10% or 60%). Bar graphs are mean ± SE of n=3-6 mice in each group. * P<0.05, ***P<0.001, as compared to the *wt* mice.

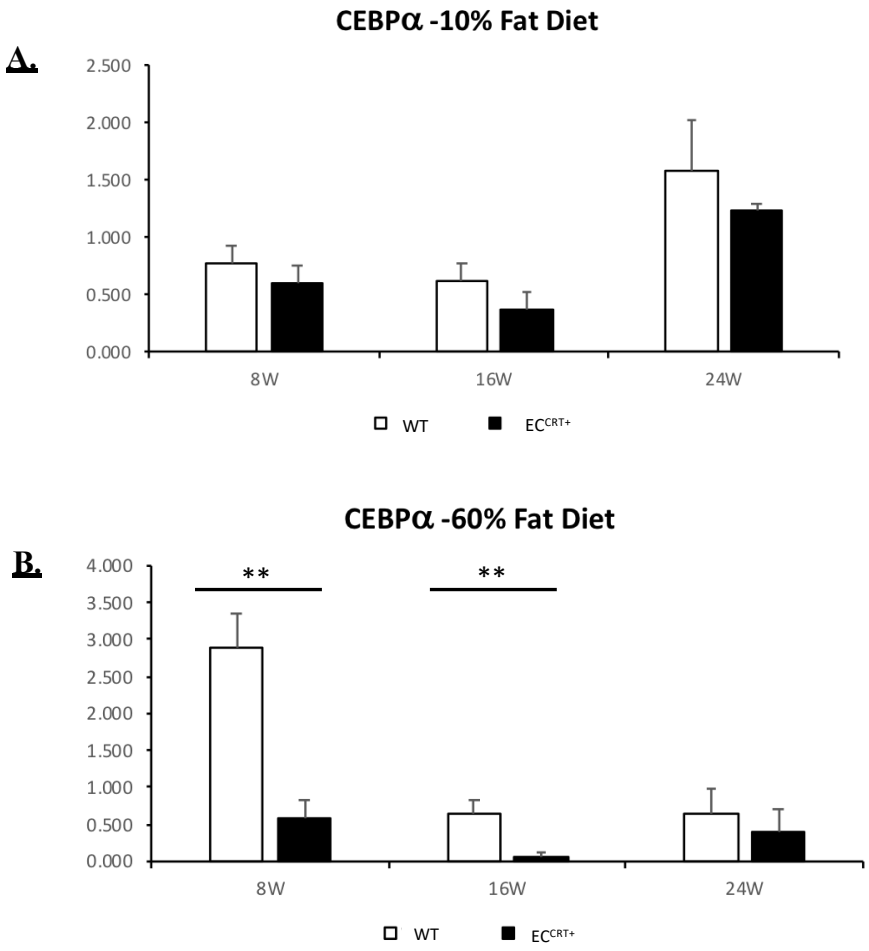

Figure 4.16 qRT-PCR of fat tissue of *EC*$^{CRT+}$ and *wt* mice under 10% and 60% fat diet. The figure shows the mRNA level of CEBPα. Downregulation of the three genes was observed on the mice under both fat diet (10% or 60%). Bar graphs are mean ± SE of n=3-6 mice in each group. ** P<0.01, as compared to the *wt* mice.

4.6 Angiogenesis in *Cdh-EC^{CRT+}-EGFP*

As previously discussed, angiogenesis plays an important role in the expansion of adipocytes and onset of obesity. In our preliminary work we have observed changes in vascular density in different tissue. Therefore, one of the objective of the current study was to measure changes in angiogenesis as one of the factors contributing to obesity. To examine the changes in the angiogenesis between the transgenic and *wt* mice, we developed *Cdh-EC^{CRT+}-EGFP* and *Cdh-EGFP* (*wt*) mice as described in Material and Methods. Cryosections of different tissues from both *Cdh-EC^{CRT+}-EGFP* and *Cdh-EGFP* mice were prepared as described in the Material and Methods. Slides were washed with PBS and mounted with mounting media containing DAPI satin and visualized directly using a Zeiss confocal microscope. The main laser line used for EGFP excitation was the argon laser at 488nm. During imaging the gain and pinhole were set constant for all images. Figure 4.17, shows representative images of sections of descending aorta, heart, mesenteric artery and visceral fat obtained from 2-3 *Cdh-EC^{CRT+}-EGFP* and *Cdh-EGFP* mice. As observed in this figure, all tissue sections from the *Cdh-EC^{CRT+}-EGFP* had a significantly higher number of endothelial cells (EGFP fluorescent, arrowheads) in comparison with *Cdh-GFP* (Figure 4.17).

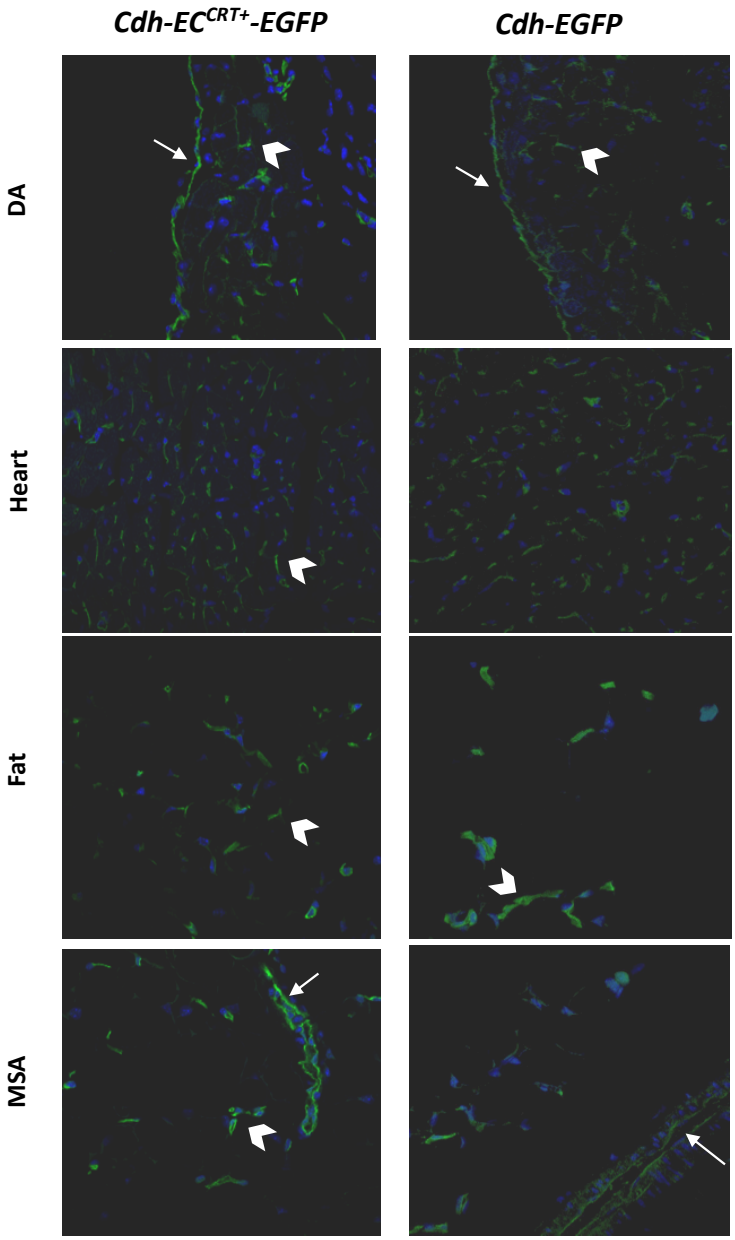

Figure 4.17 Angiogenesis analysis in *Cdh-EC^{CRT+}-EGFP*. Representative images of vasculature of different tissues obtained from *Cdh-EC^{CRT+}-EGFP* and *Cdh-EGFP* mice. Green corresponds to the endothelial cells tagged with EGFP, while blue correspond to the DAPI stain. Arrow pointing to the endothelium of the arteries. Arrowheads represents the endothelial cells in the capillaries. Images were taken using a Zeiss Confocal microscope.

CHAPTER 5. DISCUSSION

Overweight or obesity has become a public health concern worldwide. Obesity is defined as the accumulation of an abnormal or excessive fat which leads to a major health risks. Among the gulf regions, Qatar ranked sixth in obesity prevalence globally according to the international association for the study of obesity (NHS, 2012). Obesity results from an imbalance between energy intake and energy output, which is mainly associated with the adipose tissue expansion. Recently, it has been shown that adipose tissue not only stores excess energy, but it is considered to be the largest endocrine organ in the human body that exerts it effects on several other vital organs. In adults, the predominant type of fat is the subcutaneous and visceral WAT, where excess calories are stored in adipocytes as triglyceride molecules. Thus, the imbalance in energy leads to alterations in glucose and lipid disposal as well as dysregulation of adipocytokine expression in WAT. Oxidative stress and inflammation have been shown to be present in obese adipose tissue and can cause insulin resistance and adipose tissue dysfunction (Manna & Jain, 2015)

It has become well-established that maladaptive responses in the insulin resistant adipocyte can impact organelles such as the ER which is the principal site of protein synthesis and folding. ER is involved in several cellular functions in addition to protein synthesis including storage of Ca^{2+}, lipid synthesis and modification. These functions of the ER are helped by several ER resident proteins, also known as chaperones. One of the chaperones that has been shown to have multiple different functions is CRT. It plays an important role in protein folding, Ca^{2+} homeostasis, cell adhesion and lipid/phospholipid synthesis (Chaudhari et al., 2014).

As part of the quality control in the ER, CRT binds to the newly synthesized proteins and support them for correct tertiary structure folding. Improper protein folding will lead to accumulation of misfolded proteins in the ER that can activate unfolded protein response and ER stress (Rao & Bredesen, 2004). Thus, alteration in CRT expression could result in several changes in the cells. As previously mentioned that CRT could play a role in vascular development (Mesaeli et al., 1999). Like in other tissues, vasculature of adipose tissue provide oxygen, growth factors, nutrients, and cytokines to the developing tissue at different stages of tissue development and maintenance. During early development of adipose tissues, the progenitor cells receive these factors through vascular supply that help them differentiate into pre-adipocytes. Vascular endothelial cells form the inner barrier of the vessel wall and it is responsible for maintaining the vascular vasodilation and constriction. Defect in the endothelial cell function has been shown to result as a consequence of different diseases such as obesity, diabetes and high blood pressure (Lobato et al., 2012) (Singhal, 2005). An increase or decrease in the generation of reactive oxygen species is one of the causes of endothelial dysfunction (Montezano & Touyz, 2012). The fluctuation in the balance of these factors in the endothelium has an influence in the adipocyte cells which is responsible for the storage of fat which causes an impairment of adipocytes and may lead to obesity (Jankovic et al., 2016).

Various studies discussed the importance of CRT, however its role in the development of endothelial dysfunction has not been fully discussed. Furthermore, many studies have focused on how obesity induces endothelial dysfunction but, very little information is available on the role of endothelial dysfunction in the onset of obesity and diabetes. Therefore, in this study we examined the role of CRT in endothelial dysfunction and in the process of adipogenesis leading to the development of obesity and diabetes.

In our lab we have generated a mouse model that overexpressed CRT in the endothelial cells (EC^{CRT+} mice) under the control of Tie2 promoter and enhancer (Figure 3.1), which is a commonly used promoter for endothelial cells. Genotyping of the mice showed that the gene is incorporated in the mouse genome and the proteins are expressed in the arterial wall from the transgenic mice (Figure 4.1). Overall, we have observed a 20-25% increase in the CRT protein expression (Data not shown). One of the main phenotypic changes in these transgenic mice is the development of obesity and diabetes as they aged. The question which raise due to this observation was how overexpression of CRT in the endothelial cells can induce obesity? One of our initial postulate was that this could be mediated through onset of endothelial dysfunction. Indeed, De Boer et al. 2012 have reported that in obese people, impairment of endothelial function result in impair activation of endothelial nitric oxide synthase (eNOS) (De Boer et al., 2012). The reduction in eNOS reduces NO-dependent vasodilation and NO production (Hoier & Hellsten, 2014) (F. Kim et al., 2005) (Witting et al., 2007).

As shown in Figure 4.3 and 4.4, overexpression of CRT resulted in a significant reduction in eNOS expression at the level of protein and mRNA. Furthermore, previous preliminary research in our lab on the mesenteric artery function of EC^{CRT+} mice we observed a significant reduction in the relaxation of mesenteric artery in response to acetylcholine stimulation (Figure 2.3). These studies also showed that addition of NO donor (SNP) could recover the relaxation of the mesenteric artery of EC^{CRT+} mice (Figure 2.4). Overall, these data suggest the onset of endothelial dysfunction upon overexpression of CRT in the endothelial cells. Based on the previous publication we suggest that endothelial dysfunction in the EC^{CRT+} mice plays an important role in the increased obesity in these mice.

As mentioned above one of the phenotypic changes of EC^{CRT+} mice are the development of obesity and diabetes. The mice had a large volume of visceral and subcutaneous adipose tissue. Adipose tissues are the main depot for storing extra food intake as fat thus causing obesity. Development of adipose tissue is achieved through adipogensis process. Any alteration in this process could lead to obesity and many other diseases. A role for CRT in adipose cell development has been suggested (Szabo et al., 2009) but limited information is available on the effect of CRT on adipose tissue and obesity *in vivo*. To examine the phenotype of adipose tissue in the EC^{CRT+} mice, we examined sections of epididymal fat isolated from the EC^{CRT+} mice and their *wt* littermates. Interestingly, we observed a significant increase in the cell number with a decrease in cell size in the EC^{CRT+} mice as compared to the *wt* mice. This suggest that in the EC^{CRT+} mice, there is adipocyte hyperplasia not hypertrophy. Increased cell number will contribute to the increase in obesity with over-feeding. Previous reports showed that when examining

different cellular pattern in terms of various aspect of body composition, body size, and age of onset of obesity, only the latter uniquely distinguishes the hyperplastic from the hypertrophic obesity (Murphy et al., 2017)(Salans et al., 1973). Interestingly, hyperplastic obesity was characterized by an early age of onset, and hypertrophic by a late age of onset (Murphy et al., 2017). How this could be correlated to our transgenic mouse model was of interest to us. Therefore, we examined the changes in the adipocytes challenged with different fat diet. Indeed, in our mouse model they had higher adipocyte number initially suggesting early hyperplasia, as the mice aged (fed high fat diet) the adipocytes undergone hypertrophy (as seen in (Figure 4.8-4.13).

To characterize if CRT has an effect on the adipogenic process we fed 4 weeks old *wt* and transgenic (EC^{CRT+}) litter mate mice with special diet containing either high fat (60%) or regular fat (10%) diet for different time points (8-24 weeks). To ensure that the mice had similar food intake (and eliminate the possibility that one mouse line were overfeeding), they were given the same amount of food, 20 pellets of food which is equal to 20 grams of food per week. At the end time point (8, 16 or 24 weeks) glucose tolerance test (GTT) was performed to determine the state of diabetes.

Epididymal adipose tissues were collected from the *wt* and EC^{CRT+} mice for histological analysis. As shown in (Figure 4.6) there were no significant change in total body weight between the EC^{CRT+} and *wt* mice fed 10% fat diet. Similarly, there was no difference between the two-mouse line after feeding 60% fat diet. This could be attributed to the fact that we ensured equal amount of food intake by the two mouse lines. Further analysis of the body weight we observed a 65% increase in body weight in *wt* mice fed 60% fat diet while the EC^{CRT+} had increased by 94%, that is they gained more body weight

overall at 8 weeks. The same was also observed at 16 weeks (*wt* 75% and EC^{CRT+} had 98% increase) while at 24 weeks the percentage increase was reversed (*wt* 145% and EC^{CRT+} had 125% increase). Despite the observation of no changes in body weight between the two mouse lines under controlled feeding experiments, we recently received metabolomics data showing significant differences in several metabolites at each time point tested (data not shown, and currently being analyzed further).

For phenotypic analysis of the adipose tissue, we carried out the quantification of adipocyte size and numbers. As shown in Figures 4.8 to 4.13 we observed changes in the adipocyte cell size and number. Similar to our data from mice on standard chow, at 8 weeks under 10% there was a higher number of adipocyte in EC^{CRT+} with a significantly smaller size (Figure 4.8). Interestingly, as the mice aged (16 and 24 weeks on 10% fat diet), the number of cells became equal between the two mouse lines (Figure 4.9 and 4.10). This observation suggests that the hyperplasia had perhaps started at the early development and then it was maintained as the mice grew older. Figure 4.9 also illustrates that the adipocytes were still smaller in the EC^{CRT+} mice at 16 weeks after 10% fat diet, however at 24 weeks this difference was lost. This illustrates that the adipocytes of EC^{CRT+} increase in size as the mice age. After high fat diet feeding for only 8 weeks the size of the adipocyte in the EC^{CRT+} increased to the same as *wt* and interestingly there were no differences in the number of adipocytes (Figure 4.11). The same was observed for the 16 weeks. This suggest that on high fat diet there is increase in the size of adipocytes in both mice at 8 and 16 weeks.

On the other hand, after 24 weeks on 60% fat diet the number of adipocytes increased in the EC^{CRT+} mice (Figure 4.13). While, the *wt* adipocytes increased in size upon 60% fat diet for 24 weeks but the EC^{CRT+} adipocytes did not change in size (Figure 4.13). This suggest that possibly the EC^{CRT+} adipocytes have reached their maximum size.

The association between obesity and diabetes is well established. Although, not all obese will become diabetic and *vice versa*. Our results illustrated that EC^{CRT+} mice fed 60% Fat diet had more resistance to return their circulating blood glucose to normal at the end of GTT even at 8 weeks of age. This was even worse at 16 and 24 weeks (Figure 4.7). Interestingly, at 10% fat diet (regular diet) the EC^{CRT+} exhibited defect in ability to restore glucose level to normal after GTT test only at 24 weeks of feeding.

There are a number of adipogenic transcription factors and adipokines which has been shown to play an important role in the adipogenesis and can be considered as marker for adipogenesis. The peroxisome proliferator activated receptor gamma 2 (PPARγ2), CCAAT-enhancer binding protein α (CEBPα), and adiponectin are the most common adipogenic markers involved in adipose tissue development process (Miettinen et al., 2008). A study conducted by Winrow et al. 2002 showed that CRT can act as a negative regulator of PPARγ and it can also bind to GC-rich stem-loop structures causing inhibition of CEBPα mRNA translation (Winrow et al., 1995).

Szabo and colleagues showed that when CRT is overexpressed, PPARγ is downregulated suggesting again that CRT modulate PPARγ by a negative feedback mechanism (Szabo et al., 2009). Since PPARγ is consider the master regulator of the adipogenesis process, aberrant expression of CRT may alter the function of PPARγ therefore affect the adipogensis process. In this study, we showed that our EC^{CRT+} mice that overexpress CRT in endothelial cells express lower level the adipogenic markers PPARγ, and Adiponectin when fed either 10 or 60% fat diet for the different time points (8,16, and 24 weeks) (Figure 4.14 and 4.15). The effect after high fat diet was more significant. CEBPα was not different in EC^{CRT+} mice as compared to *wt* mice fed 10% diet (Figure 4.16A). However, it was significantly reduced upon feeding mice a 60% fat diet (Figure 4.16B). This suggest that the changes in the endothelial cells have an indirect effect on the adipocytes. Lemoine et al. 2013 suggested that the level of expression of several adipokines including Adiponectin are either positively or negatively correlated with the adipose area (Lemoine et al., 2013). This study supports our observation of decreased Adiponectin expression in the EC^{CRT+} mice under 10% fat diet and smaller size of the adipocyte. However, under high fat diet the increased intake of calories perhaps masked the effect of lower Adiponectin expression and the cell size was back in to different from the *wt* mice.

Finally, one of our hypothesis early in our study was a possible effect of changes in angiogenesis in the EC^{CRT+} mice as a mean to alter adipogenesis. Adipose tissue is a highly vascularized tissue and each adipocyte is surrounded by an extensive capillary network which is essential for its expansion (Lemoine et al., 2013) (Lijnen, 2008). Previous reports have showed a correlation between angiogenesis and increased adipogenesis (Lemoine et al., 2013) (Lijnen, 2008). In the current study we examined whether CRT has an effect on angiogenesis *in vivo*, using the *Cdh- EC^{CRT+}-EGFP* mice which express EGFP and overexpress CRT in the endothelial cells. Our data showed that indeed, EC^{CRT+} has a higher number of capillaries in different tissues including fat (Figure 4.17) as compared to the *wt* mice. Our result from fat, mesenteric artery and heart sections from *Cdh- EC^{CRT+}-EGFP* mice showed a significant increase in the capillaries as compared to *Cdh-EGFP* mice. The increase in the capillary number suggests activation of the angiogenesis process could be due to overexpression of CRT. In this mouse model increase in CRT and increase in angiogenesis has a very early onset (before birth). To date we do not know the time of onset of endothelial dysfunction. Our experiments to assess endothelial dysfunction were carried out on 8 weeks or older mice. It will be interesting to examine changes in endothelial function at the embryonic stage. This is one of the future line of investigation using our mouse model. Further experiments are required to confirm the correlation between the increased angiogenesis process to adipogenesis in our transgenic mouse model, however, this initial data showed a possible association between these two processes.

FUTURE DIRECTION:

1. Understand the changes in the metabolic profile of our generated transgenic and *wt* mice from the mice under diet experiment.

2. Measuring the eNOS expression level from the tissues and endothelial cells of the *Cdh- EC^{CRT+} -EGFP-* mice.

3. Increasing the number of the mice from the diet feeding experiment for quantification of adipocyte size and numbers.

LIMITATION:

Due to the limited time of the thesis submission, we were not able to finish the analysis of adipocyte phenotype in all of the mice. Thus, we were not able to complete the statistical analysis.

References

Achard, C. S., & Laybutt, D. R. (2012). Lipid-induced endoplasmic reticulum stress in liver cells results in two distinct outcomes: Adaptation with enhanced insulin signaling or insulin resistance. *Endocrinology*, *153*(5), 2164–2177. https://doi.org/10.1210/en.2011-1881

Adya, R., Tan, B. K., & Randeva, H. S. (2015). Differential effects of leptin and adiponectin in endothelial angiogenesis. *Journal of Diabetes Research*, *2015*. https://doi.org/10.1155/2015/648239

Avogaro, A., & De Kreutzenberg, S. V. (2005). Mechanisms of endothelial dysfunction in obesity. *Clinica Chimica Acta*. https://doi.org/10.1016/j.cccn.2005.04.020

Baksh, S., & Michalak, M. (1991). Expression of calreticulin in Escherichia coli and identification of its Ca2+ binding domains. *Journal of Biological Chemistry*, *266*(32), 21458–21465.

Basseri, S., Lhoták, Š., Sharma, A. M., & Austin, R. C. (2009). The chemical chaperone 4-phenylbutyrate inhibits adipogenesis by modulating the unfolded protein response. *Journal of Lipid Research*, *50*(12), 2486–2501. https://doi.org/10.1194/jlr.M900216-JLR200

Berridge, M. J., Lipp, P., & Bootman, M. D. (2000a). The versatility and universality of calcium signalling. *Nature Reviews Molecular Cell Biology*, *1*(1), 11–21. https://doi.org/10.1038/35036035

Berridge, M. J., Lipp, P., & Bootman, M. D. (2000b). The versatility and universality of calcium signalling. *Nature Reviews. Molecular Cell Biology*, *1*(1), 11–21. https://doi.org/10.1038/35036035

Boden, G. (2009). Endoplasmic reticulum stress: Another link between obesity and insulin resistance/inflammation? *Diabetes*. https://doi.org/10.2337/db08-1746

Boden, G., & Merali, S. (2011). Measurement of the increase in endoplasmic reticulum stress-related proteins and genes in adipose tissue of obese, insulin-resistant individuals. *Methods in Enzymology*, *489*(C), 67–82. https://doi.org/10.1016/B978-0-12-385116-1.00004-2

Bruemmer, D. (2012). Targeting angiogenesis as treatment for obesity. *Arteriosclerosis, Thrombosis, and Vascular Biology*, *32*(2), 161–162. https://doi.org/10.1161/ATVBAHA.111.241992

Bueter, W., Dammann, O., & Leviton, A. (2009). Endoplasmic reticulum stress, inflammation, and perinatal brain damage. *Pediatric Research*, *66*(5), 487–94. https://doi.org/10.1203/PDR.0b013e3181baa083

Caballero, A. E. (2003). Endothelial Dysfunction in Obesity and Insulin Resistance: A Road to Diabetes and Heart Disease. *Obesity Research*, *11*(11), 1278–1289. https://doi.org/10.1038/oby.2003.174

Cao, R., Brakenhielm, E., Wahlestedt, C., Thyberg, J., & Cao, Y. (2001). Leptin induces vascular permeability and synergistically stimulates angiogenesis with FGF-2 and VEGF. *Proceedings of the National Academy of Sciences of the United States of America*, *98*(11), 6390–5. https://doi.org/10.1073/pnas.101564798

Cao, Y. (2013). Angiogenesis and vascular functions in modulation of obesity, adipose metabolism, and insulin sensitivity. *Cell Metabolism*, *18*(4), 478–489. https://doi.org/10.1016/j.cmet.2013.08.008

Caramelo, J. J., Castro, O. A., Alonso, L. G., de Prat-Gay, G., & Parodi, A. J. (2003). UDP-Glc:glycoprotein glucosyltransferase recognizes structured and solvent accessible hydrophobic patches in molten globule-like folding intermediates. *Proceedings of the National Academy of Sciences*, *100*(1), 86–91. https://doi.org/10.1073/pnas.262661199

Caramelo, J. J., Castro, O. A., De Prat-Gay, G., & Parodi, A. J. (2004). The endoplasmic reticulum glucosyltransferase recognizes nearly native glycoprotein folding intermediates. *Journal of Biological Chemistry*, *279*(44), 46280–46285. https://doi.org/10.1074/jbc.M408404200

Carpio, M. A., López Sambrooks, C., Durand, E. S., & Hallak, M. E. (2010). The arginylation-dependent association of calreticulin with stress granules is regulated by calcium. *Biochemical Journal*, *429*(1), 63–72. https://doi.org/10.1042/BJ20091953

Caruso, C., Balistreri, C. R., & Candore, G. (2010). The role of adipose tissue and adipokines in obesity-related inflammatory diseases. *Mediators of Inflammation*, *2010*. https://doi.org/10.1155/2010/802078

Chan, R. S. M., & Woo, J. (2010). Prevention of overweight and obesity: How effective is the current public health approach. *International Journal of Environmental Research and Public Health*, *7*(3), 765–783. https://doi.org/10.3390/ijerph7030765

Chaudhari, N., Talwar, P., Parimisetty, A., Lefebvre dâ€™Hellencourt, C., & Ravanan, P. (2014). A Molecular Web: Endoplasmic Reticulum Stress, Inflammation, and Oxidative Stress. *Frontiers in Cellular Neuroscience*, *8*. https://doi.org/10.3389/fncel.2014.00213

Chen, Y., Wu, Z., Zhao, S., & Xiang, R. (2016). Chemical chaperones reduce ER stress and adipose tissue inflammation in high fat diet-induced mouse model of obesity. *Scientific Reports*, *6*. https://doi.org/10.1038/srep27486

Corvera, S., & Gealekman, O. (2014). Adipose tissue angiogenesis: Impact on obesity and type-2 diabetes. *Biochimica et Biophysica Acta - Molecular Basis of Disease*. https://doi.org/10.1016/j.bbadis.2013.06.003

De Boer, M. P., Meijer, R. I., Wijnstok, N. J., Jonk, A. M., Houben, A. J., Stehouwer, C. D., … Serné, E. H. (2012). Microvascular Dysfunction: A Potential Mechanism in the Pathogenesis of Obesity-associated Insulin Resistance and Hypertension. *Microcirculation*. https://doi.org/10.1111/j.1549-8719.2011.00130.x

Decca, M. B., Carpio, M. A., Bosc, C., Galiano, M. R., Job, D., Andrieux, A., & Hallak, M. E. (2007). Post-translational arginylation of calreticulin: A new isospecies of calreticulin component of stress granules. *Journal of Biological Chemistry*, *282*(11), 8237–8245. https://doi.org/10.1074/jbc.M608559200

Dedhar, S. (1994). Novel functions for calreticulin: Interaction with integrins and modulation of gene expression? *Trends in Biochemical Sciences*. https://doi.org/10.1016/0968-0004(94)90001-9

Denzel, A., Molinari, M., Trigueros, C., Martin, J. E., Velmurgan, S., Brown, S., … Owen, M. J. (2002). Early postnatal death and motor disorders in mice congenitally deficient in calnexin expression. *Molecular and Cellular Biology*, *22*(21), 7398–7404. https://doi.org/10.1128/MCB.22.21.7398-7404.2002

Dupuis, B. M., Schaerer, E., Krause, K., & Tschopp, J. (1993). The Calcium-binding Protein Calreticulin Is a Major Constituent of Lytic Granules in Cytolytic T Lymphocytes. *Journal of Experimental Medicine*, *177*(January), 1–7. https://doi.org/10.1084/jem.177.1.1

Farnier, C., Krief, S., Blache, M., Diot-Dupuy, F., Mory, G., Ferre, P., & Bazin, R. (2003). Adipocyte functions are modulated by cell size change: potential involvement of an integrin/ERK signalling pathway. *International Journal of Obesity*, *27*(10), 1178–1186. https://doi.org/10.1038/sj.ijo.0802399

Frickel, E.-M., Riek, R., Jelesarov, I., Helenius, A., Wuthrich, K., & Ellgaard, L. (2002). TROSY-NMR reveals interaction between ERp57 and the tip of the calreticulin P-domain. *Proceedings of the National Academy of Sciences*, *99*(4), 1954–1959. https://doi.org/10.1073/pnas.042699099

Fu, S., Yang, L., Li, P., Hofmann, O., Dicker, L., Hide, W., … Hotamisligil, G. S. (2011). Aberrant lipid metabolism disrupts calcium homeostasis causing liver endoplasmic reticulum stress in obesity. *Nature*, *473*(7348), 528–531. https://doi.org/10.1038/nature09968

Garg, A. (2011). Lipodystrophies: Genetic and acquired body fat disorders. *Journal of Clinical Endocrinology and Metabolism*. https://doi.org/10.1210/jc.2011-1159

Giraldo, A. M. V., Medus, M. L., Lebrero, M. G., Pagano, R. S., Labriola, C. A., Landolfo, L., … Caramelo, J. J. (2010). The structure of calreticulin C-terminal domain is modulated by physiological variations of calcium concentration. *Journal of Biological Chemistry*, *285*(7), 4544–4553. https://doi.org/10.1074/jbc.M109.034512

Gold, L. I., Eggleton, P., Sweetwyne, M. T., Van Duyn, L. B., Greives, M. R., Naylor, S.-M., … Murphy-Ullrich, J. E. (2010). Calreticulin: non-endoplasmic reticulum functions in physiology and disease. *The FASEB Journal*, *24*(3), 665–683. https://doi.org/10.1096/fj.09-145482

Gregoire, F. M., Smas, C. M., & Sul, H. S. (1998). Understanding adipocyte differentiation. *Physiological Reviews*, *78*(3), 783–809. https://doi.org/10.1074/jbc.272.8.5128

Gregor, M. F., & Hotamisligil, G. S. (2007a). Adipocyte stress: the endoplasmic reticulum and metabolic disease. *Journal of Lipid Research*, *48*(9), 1905–1914. https://doi.org/10.1194/jlr.R700007-JLR200

Gregor, M. F., & Hotamisligil, G. S. (2007b). Thematic review series: Adipocyte Biology. Adipocyte stress: the endoplasmic reticulum and metabolic disease. *Journal of Lipid Research*, *48*, 1905–1914. https://doi.org/10.1194/jlr.R700007-JLR200

Hammond, C., Braakman, I., & Helenius, A. (1994). Role of N-linked oligosaccharide recognition, glucose trimming, and calnexin in glycoprotein folding and quality control. *Proceedings of the National Academy of Sciences*, *91*(3), 913–917. https://doi.org/10.1073/pnas.91.3.913

Han, S., Sun, H. M., Hwang, K.-C., & Kim, S.-W. (2015). Adipose-Derived Stromal Vascular Fraction Cells: Update on Clinical Utility and Efficacy. *Critical Reviews in Eukaryotic Gene Expression*, *25*(2), 145–52. https://doi.org/10.1615/CritRevEukaryotGeneExpr.2015013057

Hebert, D. N., & Molinari, M. (2007). In and Out of the ER: Protein Folding, Quality Control, Degradation, and Related Human Diseases. *Physiological Reviews*, *87*(4), 1377–1408. https://doi.org/10.1152/physrev.00050.2006

Helenius, A. (2001). Intracellular Functions of N-Linked Glycans. *Science*, *291*(5512), 2364–2369. https://doi.org/10.1126/science.291.5512.2364

Hoier, B., & Hellsten, Y. (2014). Exercise-induced capillary growth in human skeletal muscle and the dynamics of VEGF. *Microcirculation*. https://doi.org/10.1111/micc.12117

Ihara, Y., Kageyama, K., & Kondo, T. (2005). Overexpression of calreticulin sensitizes SERCA2a to oxidative stress. *Biochemical and Biophysical Research Communications*, *329*(4), 1343–1349. https://doi.org/10.1016/j.bbrc.2005.02.112

Jankovic, A., Korac, A., Buzadzic, B., Stancic, A., Otasevic, V., Ferdinandy, P., … Korac, B. (2016). Targeting the nitric oxide/superoxide ratio in adipose tissue: relevance in obesity and diabetes management. *British Journal of Pharmacology*, *174*, 1570–1590. https://doi.org/10.1111/bph.13498

Jeffery, E., Peters, L. R., & Raghavan, M. (2011). The polypeptide binding conformation of calreticulin facilitates its cell-surface expression under conditions of endoplasmic reticulum stress. *Journal of Biological Chemistry*, *286*(4), 2402–2415. https://doi.org/10.1074/jbc.M110.180877

Jiang, Y., Dey, S., & Matsunami, H. (2014). Calreticulin: Roles in cell-surface protein expression. *Membranes*, *4*(3), 630–641. https://doi.org/10.3390/membranes4030630

Jo, J., Gavrilova, O., Pack, S., Jou, W., Mullen, S., Sumner, A. E., … Periwal, V. (2009). Hypertrophy and/or hyperplasia: Dynamics of adipose tissue growth. *PLoS Computational Biology*, *5*(3). https://doi.org/10.1371/journal.pcbi.1000324

Jorgensen, C. S., Trandum, C., Larsen, N., Ryder, L. R., Gajhede, M., Skov, L. K., … Houen, G. (2005). Conformational stability of calreticulin. *Protein Pept Lett*, *12*(7), 687–693. https://doi.org/10.2174/0929866054696082

Kapoor, M., Srinivas, H., Kandiah, E., Gemma, E., Ellgaard, L., Oscarson, S., … Surolia, A. (2003). Interactions of substrate with calreticulin, an endoplasmic reticulum chaperone. *Journal of Biological Chemistry*, *278*(8), 6194–6200. https://doi.org/10.1074/jbc.M209132200

Katz, a J., Llull, R., Hedrick, M. H., & Futrell, J. W. (1999). Emerging approaches to the tissue engineering of fat. *Clinics in Plastic Surgery*.

Keller, S. H., Lindstrom, J., & Taylor, P. (1998). Inhibition of glucose trimming with castanospermine reduces calnexin association and promotes proteasome degradation of the ??-subunit of the nicotinic acetylcholine receptor. *Journal of Biological Chemistry*, *273*(27), 17064–17072. https://doi.org/10.1074/jbc.273.27.17064

Kim, F., Tysseling, K. a, Rice, J., Pham, M., Haji, L., Gallis, B. M., … Raines, E. W. (2005). Free fatty acid impairment of nitric oxide production in endothelial cells is mediated by IKKbeta. *Arteriosclerosis, Thrombosis, and Vascular Biology*, *25*(5), 989–94. https://doi.org/10.1161/01.ATV.0000160549.60980.a8

Kim, J. A., Montagnani, M., Kwang, K. K., & Quon, M. J. (2006). Reciprocal relationships between insulin resistance and endothelial dysfunction: Molecular and pathophysiological mechanisms. *Circulation*. https://doi.org/10.1161/CIRCULATIONAHA.105.563213

Kolluru, G. K., Bir, S. C., & Kevil, C. G. (2012). Endothelial dysfunction and diabetes: Effects on angiogenesis, vascular remodeling, and wound healing. *International Journal of Vascular Medicine*, *2012*(Figure 1). https://doi.org/10.1155/2012/918267

Konieczny, S. F., & Emerson, C. P. (1984). 5-azacytidine induction of stable mesodermal stem cell lineages from 10T1/2 cells: Evidence for regulatory genes controlling determination. *Cell*, *38*(3), 791–800. https://doi.org/10.1016/0092-8674(84)90274-5

Kraus, A., Groenendyk, J., Bedard, K., Baldwin, T. A., Krause, K. H., Dubois-Dauphin, M., … Michalak, M. (2010). Calnexin deficiency leads to dysmyelination. *Journal of Biological Chemistry*, *285*(24), 18928–18938. https://doi.org/10.1074/jbc.M110.107201

Leach, M. R., Cohen-Doyle, M. F., Thomas, D. Y., & Williams, D. B. (2002). Localization of the lectin, ERp57 binding, and polypeptide binding sites of calnexin and calreticulin. *Journal of Biological Chemistry*, *277*(33), 29686–29697. https://doi.org/10.1074/jbc.M202405200

Lemoine, A. Y., Ledoux, S., & Larger, E. (2013). Adipose tissue angiogenesis in obesity. *Thrombosis and Haemostasis*, *110*(4), 661–669. https://doi.org/10.1160/TH13-01-0073

Lijnen, H. R. (2008). Angiogenesis and obesity. *Cardiovascular Research*, *78*(2), 286–293. https://doi.org/10.1093/cvr/cvm007

Lobato, N. S., Filgueira, F. P., Akamine, E. H., Tostes, R. C., Carvalho, M. H. C., & Fortes, Z. B. (2012). Mechanisms of endothelial dysfunction in obesity-associated hypertension. *Brazilian Journal of Medical and Biological Research*, *45*(5), 392–400. https://doi.org/10.1590/S0100-879X2012007500058

Mandrup, S., Loftus, T. M., MacDougald, O. A., Kuhajda, F. P., & Lane, M. D. (1997). Obese gene expression at in vivo levels by fat pads derived from s.c. implanted 3T3-F442A preadipocytes. *Proceedings of the National Academy of Sciences of the United States of America*, *94*(9), 4300–4305. https://doi.org/10.1073/pnas.94.9.4300

Manna, P., & Jain, S. K. (2015). Obesity, Oxidative Stress, Adipose Tissue Dysfunction, and the Associated Health Risks: Causes and Therapeutic Strategies. *Metabolic Syndrome and Related Disorders*, *13*(10), 423–444. https://doi.org/10.1089/met.2015.0095

McCauliffe, D. P., Yang, Y. S., Wilson, J., Sontheimer, R. D., & Capra, J. D. (1992). The 5'-flanking region of the human calreticulin gene shares homology with the human GRP78, GRP94, and protein disulfide isomerase promoters. *Journal of Biological Chemistry*, *267*(4), 2557–2562.

Mery, L., Mesaeli, N., Michalak, M., Opas, M., Lew, D. P., & Krause, K. H. (1996). Overexpression of calreticulin increases intracellular Ca2+ storage and decreases store-operated Ca2+ influx. *Journal of Biological Chemistry*, *271*(16), 9332–9339. https://doi.org/10.1074/jbc.271.16.9332

Mesaeli, N., Nakamura, K., Zvaritch, E., Dickie, P., Dziak, E., Krause, K. H., … Michalak, M. (1999). Calreticulin is essential for cardiac development. *Journal of Cell Biology*, *144*(5), 857–868. https://doi.org/10.1083/jcb.144.5.857

Michalak, M., Corbett, E. F., Mesaeli, N., Nakamura, K., & Opas, M. (1999). Calreticulin: one protein, one gene, many functions. *The Biochemical Journal*, *344 Pt 2*, 281–92. https://doi.org/10.1042/BJ3440281

Michalak, M., Groenendyk, J., Szabo, E., Gold, L. I., & Opas, M. (2009). Calreticulin, a multi-process calcium-buffering chaperone of the endoplasmic reticulum. *Biochemical Journal*, *417*(3), 651–666. https://doi.org/10.1042/BJ20081847

Michalak, M., Parker, J. M. R., & Opas, M. (2002). Ca2+ signaling and calcium binding chaperones of the endoplasmic reticulum. *Cell Calcium*. https://doi.org/10.1016/S0143416002001884

Miettinen, S., Sarkanen, J. R., & Ashammakhi, N. (2008a). Adipose Tissue and Adipocyte. *Topics in Tissue Engineering*, *4*, 1–26.

Miettinen, S., Sarkanen, J. R., & Ashammakhi, N. (2008b). Adipose Tissue and Adipocyte Differentiation: Molecular and Cellular Aspects and Tissue Engineering Applications. *Topics in Tissue Engineering*, *4*, 1–26.

Molinari, M., Eriksson, K. K., Calanca, V., Galli, C., Cresswell, P., Michalak, M., & Helenius, A. (2004). Contrasting Functions of Calreticulin and Calnexin in Glycoprotein Folding and ER Quality Control. *Molecular Cell*, *13*(1), 125–135. https://doi.org/10.1016/S1097-2765(03)00494-5

Montagnani, M., Ravichandran, L. V, Chen, H., Esposito, D. L., & Quon, M. J. (2002). Insulin receptor substrate-1 and phosphoinositide-dependent kinase-1 are required for insulin-stimulated production of nitric oxide in endothelial cells. *Molecular Endocrinology (Baltimore, Md.)*, *16*(8), 1931–42. https://doi.org/10.1210/me.2002-0074

Montezano, A. C., & Touyz, R. M. (2012). Reactive oxygen species and endothelial function--role of nitric oxide synthase uncoupling and Nox family nicotinamide adenine dinucleotide phosphate oxidases. *Basic & Clinical Pharmacology & Toxicology*, *110*(1), 87–94. https://doi.org/10.1111/j.1742-7843.2011.00785.x

Murphy, J., Moullec, G., & Santosa, S. (2017). Factors associated with adipocyte size reduction after weight loss interventions for overweight and obesity: a systematic review and meta-regression. *Metabolism*, *67*, 31–40. https://doi.org/10.1016/j.metabol.2016.09.009

Neels, J. G., Thinnes, T., & Loskutoff, D. J. (2004). Angiogenesis in an in vivo model of adipose tissue development. *FASEB Journal : Official Publication of the Federation of American Societies for Experimental Biology*, *18*(9), 983–5. https://doi.org/10.1096/fj.03-1101fje

NHS. (2012). Qatar Health Report 2012, 1–34. Retrieved from http://www.nhsq.info/app/media/1479

Oliver, J. D., Van Der Wal, F. J., Bulleid, N. J., & High, S. (1997). Interaction of the thiol-dependent reductase ERp57 with nascent glycoproteins. *Science*, *275*(5296), 86–88. https://doi.org/10.1126/science.275.5296.86

Onat, D., Brillon, D., AM, S., & PC, C. (2012). Human Vascular Endothelial Cells: A Model System for Studying Vascular Inflammation in Diabetes and Atherosclerosis. *Curr Diab Rep*, *11*(3), 193–202. https://doi.org/10.1007/s11892-011-0182-2.Human

Opas, M., Szewczenko-Pawlikowski, M., Jass, G. K., Mesaeli, N., & Michalak, M. (1996). Calreticulin modulates cell adhesiveness via regulation of vinculin expression. *Journal of Cell Biology*, *135*(6 II), 1913–1923. https://doi.org/10.1083/jcb.135.6.1913

Ostwald, T. J., & MacLennan, D. H. (1974). Isolation of a High Affinity Calcium-binding Protein from Sarcoplasmic Reticulum. *Journal of Biological Chemistry* , *249*(3), 974–979. Retrieved from http://www.jbc.org/content/249/3/974.abstract

Ozcan, L., & Tabas, I. (2012). Role of Endoplasmic Reticulum Stress in Metabolic Disease and Other Disorders. *Annual Review of Medicine*, *63*(1), 317–328. https://doi.org/10.1146/annurev-med-043010-144749

Ozcan, U., Cao, Q., Yilmaz, E., Lee, A.-H., Iwakoshi, N. N., Ozdelen, E., … Hotamisligil, G. S. (2004). Endoplasmic reticulum stress links obesity, insulin action, and type 2 diabetes. *Science (New York, N.Y.)*, *306*(5695), 457–461. https://doi.org/10.1126/science.1103160

Peters, L. R., & Raghavan, M. (2011). Endoplasmic Reticulum Calcium Depletion Impacts Chaperone Secretion, Innate Immunity, and Phagocytic Uptake of Cells. *The Journal of Immunology*, *187*(2), 919–931. https://doi.org/10.4049/jimmunol.1100690

Peterson, J. R., Ora, A., Van, P. N., & Helenius, A. (1995). Transient, lectin-like association of calreticulin with folding intermediates of cellular and viral glycoproteins. *Molecular Biology of the Cell*, *6*(9), 1173–84. https://doi.org/10.1091/mbc.6.9.1173

Pipe, S. W., Morris, J. A., Shah, J., & Kaufman, R. J. (1998). Differential interaction of coagulation factor VIII and factor V with protein chaperones calnexin and calreticulin. *Journal of Biological Chemistry*, *273*(14), 8537–8544. https://doi.org/10.1074/jbc.273.14.8537

Potenza, M. A., Marasciulo, F. L., Chieppa, D. M., Brigiani, G. S., Formoso, G., Quon, M. J., & Montagnani, M. (2005). Insulin resistance in spontaneously hypertensive rats is associated with endothelial dysfunction characterized by imbalance between NO and ET-1 production. *American Journal of Physiology. Heart and Circulatory Physiology*, *289*(2), H813-22. https://doi.org/10.1152/ajpheart.00092.2005

Prattes, S., Hörl, G., Hammer, A., Blaschitz, A., Graier, W. F., Sattler, W., … Steyrer, E. (2000). Intracellular distribution and mobilization of unesterified cholesterol in adipocytes: triglyceride droplets are surrounded by cholesterol-rich ER-like surface layer structures. *Journal of Cell Science*, *113 (Pt 1*, 2977–2989.

Prieto, D., Contreras, C., & Sánchez, A. (2014). Endothelial dysfunction, obesity and insulin resistance. *Current Vascular Pharmacology*, *12*(3), 412–26. https://doi.org/10.2174/15701611126661404232210008

Rao, R. V., & Bredesen, D. E. (2004). Misfolded proteins, endoplasmic reticulum stress and neurodegeneration. *Current Opinion in Cell Biology*. https://doi.org/10.1016/j.ceb.2004.09.012

Roderick, H. L., Lechleiter, J. D., & Camacho, P. (2000). Cytosolic phosphorylation of calnexin controls intracellular Ca2+ oscillations via an interaction with SERCA2b. *Journal of Cell Biology*, *149*(6), 1235–1247. https://doi.org/10.1083/jcb.149.6.1235

Rooke, K., Briquet-Laugier, V., Xia, Y. R., Lusis, A. J., & Doolittle, M. H. (1997). Mapping of the gene for calreticulin (Calr) to mouse chromosome 8. *Mammalian Genome*, *8*(11), 870–871. https://doi.org/10.1007/s003359900599

Rupnick, M. A., Panigrahy, D., Zhang, C.-Y., Dallabrida, S. M., Lowell, B. B., Langer, R., & Folkman, M. J. (2002). Adipose tissue mass can be regulated through the vasculature. *Proceedings of the National Academy of Sciences*, *99*(16), 10730–10735. https://doi.org/10.1073/pnas.162349799

Salans, L. B., Cushman, S. W., & Weismann, R. E. (1973). Studies of human adipose tissue. Adipose cell size and number in nonobese and obese patients. *The Journal of Clinical Investigation*, *52*(4), 929–941. https://doi.org/10.1172/JCI107258

Sambrooks, C. L., Carpio, M. A., & Hallak, M. E. (2012). Arginylated calreticulin at plasma membrane increases susceptibility of cells to apoptosis. *Journal of Biological Chemistry*, *287*(26), 22043–22054. https://doi.org/10.1074/jbc.M111.338335

Schrag, J. D., Bergeron, J. J. M., Li, Y., Borisova, S., Hahn, M., Thomas, D. Y., & Cygler, M. (2001). The structure of calnexin, an ER chaperone involved in quality control of protein folding. *Molecular Cell*, *8*(3), 633–644. https://doi.org/10.1016/S1097-2765(01)00318-5

Serge Arnaudeau, Maud Frieden, Kim Nakamura, Cyril Castelbou, Marek Michalak, and N. D. (2002). Calreticulin Differentially Modulates Calcium Uptake and Release in the Endoplasmic Reticulum and Mitochondria*, *277*(48), 46696–46705. https://doi.org/10.1074/jbc.M202395200

Sharma, N. K., Das, S. K., Mondal, A. K., Hackney, O. G., Chu, W. S., Kern, P. A., … Elbein, S. C. (2008). Endoplasmic reticulum stress markers are associated with obesity in nondiabetic subjects. *The Journal of Clinical Endocrinology and Metabolism*, *93*(11), 4532–4541. https://doi.org/10.1210/jc.2008-1001

Sierra-Honigmann, M. R. (1998). Biological Action of Leptin as an Angiogenic Factor. *Science*, *281*(5383), 1683–1686. https://doi.org/10.1126/science.281.5383.1683

Singhal, A. (2005). Endothelial dysfunction: role in obesity-related disorders and the early origins of CVD. *Proceedings of the Nutrition Society*, *64*(1), 15–22. https://doi.org/10.1079/PNS2004404

Spiro, R. G., Zhu, Q., Bhoyroo, V., & Söling, H. D. (1996). Definition of the lectin-like properties of the molecular chaperone, calreticulin, and demonstration of its copurification with endomannosidase from rat liver Golgi. *Journal of Biological Chemistry*, *271*(19), 11588–11594. https://doi.org/10.1074/jbc.271.19.11588

Szabo, E., Feng, T., Dziak, E., & Opas, M. (2009). Cell adhesion and spreading affect adipogenesis from embryonic stem cells: The role of calreticulin. *Stem Cells*, *27*(9), 2092–2102. https://doi.org/10.1002/stem.137

Tang, W., Zeve, D., Suh, J. M., Bosnakovski, D., Kyba, M., Hammer, R. E., … Graff, J. M. (2008). White Fat Progenitor Cells Reside in the Adipose Vasculature. *Science*, *322*(5901), 583–586. https://doi.org/10.1126/science.1156232

Tchkonia, T., Thomou, T., Zhu, Y., Karagiannides, I., Pothoulakis, C., Jensen, M. D., & Kirkland, J. L. (2013). Mechanisms and metabolic implications of regional differences among fat depots. *Cell Metabolism*. https://doi.org/10.1016/j.cmet.2013.03.008

Trayhurn, P., & Beattie, J. H. (2001). Physiological role of adipose tissue: white adipose tissue as an endocrine and secretory organ. *Proceedings of the Nutrition Society*, *60*(3), 329–339. https://doi.org/10.1079/PNS200194

Trombetta, E. S., Simons, J. F., & Helenius, A. (1996). Endoplasmic reticulum glucosidase II is composed of a catalytic subunit, conserved from yeast to mammals, and a tightly bound noncatalytic HDEL- containing subunit. *Journal of Biological Chemistry*, *271*(44), 27509–27516. https://doi.org/10.1074/jbc.271.44.27509

Wada, I., Imai, S. I., Kai, M., Sakane, F., & Kanoh, H. (1995). Chaperone function of calreticulin when expressed in the endoplasmic reticulum as the membrane-anchored and soluble forms. *Journal of Biological Chemistry*. https://doi.org/10.1074/jbc.270.35.20298

White, T. K., Zhu, Q., & Tanzer, M. L. (1995). Cell surface calreticulin is a putative mannoside lectin which triggers mouse melanoma cell spreading. *Journal of Biological Chemistry*, *270*(27), 15926–15929. https://doi.org/10.1074/jbc.270.27.15926

WHO. (2012). WHO | Obesity and overweight. *World Health Organisation Media Centre Fact Sheet No. 311*, 1–2. Retrieved from http://www.who.int/mediacentre/factsheets/fs311/en/#.U2gDIH5zIZ4.mendeley

Wilcox, G. (2005). Insulin and insulin resistance. *The Clinical Biochemist. Reviews / Australian Association of Clinical Biochemists*, *26*(2), 19–39. https://doi.org/10.1016/S0025-7125(03)00128-7

Winrow, C. J., Miyata, K. S., Marcus, S. L., Burns, K., Michalak, M., Capone, J. P., & Rachubinski, R. A. (1995). Calreticulin Modulates the in-Vitro DNA-Binding but Not the in-Vivo Transcriptional Activation by Peroxisome Proliferator-Activated Receptor Retinoid-X Receptor Heterodimers. *Molecular and Cellular Endocrinology*, *111*(2), 175–179.

Witting, P. K., Rayner, B. S., Wu, B. J., Ellis, N. A., & Stocker, R. (2007). Hydrogen peroxide promotes endothelial dysfunction by stimulating multiple sources of superoxide anion radical production and decreasing nitric oxide bioavailability. *Cellular Physiology and Biochemistry*, *20*(5), 255–268. https://doi.org/10.1159/000107512

Xue, Y., Petrovic, N., Cao, R., Larsson, O., Lim, S., Chen, S., … Cao, Y. (2009). Hypoxia-Independent Angiogenesis in Adipose Tissues during Cold Acclimation. *Cell Metabolism*, *9*(1), 99–109. https://doi.org/10.1016/j.cmet.2008.11.009

Yokoyama, M., & Hirata, K. I. (2005). New function of calreticulin: Calreticulin-dependent mRNA destabilization. *Circulation Research*, *97*(10), 961–963. https://doi.org/10.1161/01.RES.0000193564.46466.2a

Zapun, A., Darby, N. J., Tessier, D. C., Michalak, M., Bergeron, J. J. M., & Thomas, D. Y. (1998). Enhanced catalysis of ribonuclease B folding by the interaction of calnexin or calreticulin with ERp57. *Journal of Biological Chemistry*, *273*(11), 6009–6012. https://doi.org/10.1074/jbc.273.11.6009

Zeng, G., Nystrom, F. H., Ravichandran, L. V., Cong, L. N., Kirby, M., Mostowski, H., & Quon, M. J. (2000). Roles for insulin receptor, PI3-kinase, and Akt in insulin-signaling pathways related to production of nitric oxide in human vascular endothelial cells. *Circulation*, *101*(13), 1539–1545. https://doi.org/10.1161/01.CIR.101.13.1539

APPENDIX A: Ethical Approval

Weill Cornell Medicine-Qatar

Institutional Animal Care and Use Committee

To:	Mesaeli, Nasrin
From:	Dr. Hani Najafi
	Institutional Animal Care and Use Committee (IACUC)
Date:	May 15, 2017
Subject:	IACUC Approval Notification
Project Title:	Regulation of vascular wall remodeling by endoplasmic reticulum

Your Protocol has been approved.

Approval Date:	May 15, 2017
Protocol Number:	2012-0031
Request:	Annual Renewal
Personnel Listed:	Mesaeli, Nasrin; Conti, Cindy; Dalloul, Rajaa S. D.; Lobo, Tatiana Correa Carneiro; Massaeli, Hamid; Talaber, Cheryl Little

The following grant/sponsored project application(s) associated with this IACUC protocol was/were reviewed and the IACUC confirms that the research involving animals specified in the application(s) listed below is approved.

Grant sponsored Project PI:	Mesaeli, Nasrin
Grant sponsored Project Title:	Role of Endothelial Dysfunction in the Etiology of Diabetes and Metabolic Syndrome
Grant sponsored Project Number:	NPRP 7-208-3-046
Grant Agency/Sponsor:	Qatar National Research Fund

Species Use	Category C	Category D	Category E
Experimental Plan for Mice	3536	0	0

The request for annual renewal of the above protocol was reviewed and approved by the WCM-Q Institutional Animal Care and Use Committee for the period of one year.

Please forward a copy of this IACUC correspondence to all co-investigators on your project.

Signature

Hani Najafi, Ph.D.
IACUC Alternate Chair
Assistant Professor of Cell & Developmental Biology
Weill Cornell Medicine in Qatar

WCMC-Q RESEARCH DIVISION

Cc.
Khaled Machaca, PhD
Associate Dean for Research
Organizational Official
Weill Cornell Medicine in Qatar

Page 1 of 1

APPENDIX B: Abstract translated in Arabic

خلل داخل بطانة الأوعية الدموية كآلية تتسبب في تطوير السمنة

تعتبر السمنة واحدة من أهم قضايا الصحة العامة في العالم مع زيادة سريعة في انتشارها. ووفقاً لآخر تقرير من الصحة العامة العليا في قطر في عام 2012، كانت نسبة البدانة لدى النساء 71.8٪ مقارنة بـ 68.3٪ لدى الرجال. الخلايا الدهنية هي حيث يمكن أن يختلف حجمها باختلاف مدخول الطعام. التوسع السريع في الأنسجة الدهنية يتطلب وجود أوعية دموية عالية لدعم توسعها. تفرع الأوعية الدموية يعتمد على عمل الخلايا البطانية بشكل صحيح. تم اصدار العديد من التقارير عن أمراض مختلفة بما في ذلك مرض السكري والسمنة والتي كان سببها عيوب في وظيفة الخلية البطانية. يمكن أن يكون هذا العيب بسبب التغيرات في إنتاج النيتريك أكسيد الذي ينظم انقباض الأوعية الدموية أو إنتاج الأوكسيراديكالس الأخرى مما يؤدي إلى تلف الأنسجة.

Calreticulin (CRT) هو بروتين متعدد الوظائف يوجد في الشبكة الاندوبلازمية لكل خلايا الثدييات. الوظائف الرئيسية لهذا البروتين هي تنظيم الخلايا. أظهر نموذج الفئران المعدلة وراثيا في هذه الدراسة overexpressed CRT في الخلايا البطانية (EC^{CRT+})أدلة على خلل وظيفي في الخلايا البطانية والقابلية للسمنة ومرض السكري مع تقدم هذه الفئران في السن. لذلك، افترضنا أن الإفراط في CRT في الخلايا البطانية يؤدي إلى خلل وظيفي بطاني يزيد من التفرع الوعائي مما يؤدي إلى تنشيط عملية تكوين الدهون.

في هذه الدراسة درسنا التغييرات الظاهرية في الوزن للخلايا الدهنية في كلاً من الفئران *wt* و EC^{CRT+} حيث تمت تغذيتهم الدهون (60 ٪) أو الدهون العادية (10 ٪) لفترة زمنية مختلفة (24-8 أسابيع). أظهرت النتائج التي توصلنا إليها أن هذه الفئران لديها نسبة eNOS أقل من الطبيعي مما يؤدي إلى ضعف في وظيفة الخلايا البطانية. أوضحت فحوصات السكر في الدم GTT أن فئران EC^{CRT+} طورت مرض السكري مع تقدم العمر عند تناول 10٪ من الدهون. ومع ذلك، على نظام غذائي غني بالدهون فشلوا في تنظيم مستوي السكر في الدم حتى في 8 أسابيع. أظهر التحليل النسيجي للوزن لكلاً من الفئران EC^{CRT+} و *wt* تغييرات كبيرة في حجم الخلايا الدهنية وعددها لما يشير إلى وجود ارتباط بين زيادة بروتين CRT في الخلايا البطانية والخلل الذي تسبب في خلل وظيفتها وبين وظيفة تكوين الدهون. دراستنا هي الأولى التي تظهر الدور المهم لخلل وظيفة الخلاية الباطنية في تغيير عملية تكوين الدهون التي تؤدي إلى تطور السمنة ومرض السكري. كما تسلط بياناتنا الضوء على أهمية وجود البروتينات الموجودة في الشبكة الاندوبلازمية في هذه العملية.